© 2024 Journal of Pharmacy & Pharmacognosy Research, 12 (5), 972-993, 2024
ISSN 0719-4250
https://jppres.com

DOI: https://doi.org/10.56499/jppres24.1956_12.5.972

Original Article

Anti-inflammatory effect of the mixture of *Ageratum conyzoides* L. extract and eggshell membrane hydrolysates and *in silico* active compound predictions

[Efecto antiinflamatorio de la mezcla de extracto de *Ageratum conyzoides* L. e hidrolizados de membrana de cáscara de huevo, y predicción *in silico* de compuestos activos]

Suci Nar Vikasari[1,3*], Elin Yulinah Sukandar[3], Tri Suciati[2], I Ketut Adnyana[1*]

[1]Department of Pharmacology and Clinical Pharmacy, School of Pharmacy, Bandung Institute of Technology, Bandung, Indonesia.
[2]Department of Pharmaceutics, School of Pharmacy, Bandung Institute of Technology, Bandung, Indonesia.
[3]Department of Pharmacology and Clinical Pharmacy, Faculty of Pharmacy, Universitas Jenderal Achmad Yani, Cimahi, Indonesia.
*E-mail: uci.vikasari@lecture.unjani.ac.id; ketut@itb.ac.id

Abstract

Context: *Ageratum conyzoides* L. and eggshell membrane have the potential to be used as medicine. The independent use of *A. conyzoides* extract or eggshell membrane hydrolysates independently as a natural medicine has been widely known, but the mixture of the two as an anti-inflammatory has not been studied.

Aims: To evaluate both the *in vivo* and *in vitro* anti-inflammatory effects of *A. conyzoides* extract and eggshell membrane hydrolysates, independently and in combination. *In silico* testing was conducted to identify chemicals that have a key role in inflammation signaling pathways.

Methods: The chronic anti-inflammatory effects of *A. conyzoides* extract and eggshell membrane hydrolysates were evaluated on cotton pellet-induced rats using diclofenac-Na as a control. *In vitro* anti-inflammatory effects were studied via protein denaturation, membrane stability, and antiprotease activity. Furthermore, molecular docking was performed on the p38-MAPK signaling pathway using compounds found in *A. conyzoides* extract and eggshell membrane hydrolysates.

Results: *A. conyzoides* extract and eggshell membrane hydrolysates given separately or in combination can inhibit the formation of exudates and granulomas. Molecular docking simulations showed that the metabolites in the extract and hydrolysate interact with p38-MAPK. Nobiletin in the extract is the potential metabolite that interacts with the p38-MAPK receptor with a free energy of binding and inhibition constant of -8.92 kcal/mol and 260.80 nM. Amino acids in the hydrolysates showed weaker interactions compared to the compound in the extract.

Conclusions: *A. conyzoides* extract and eggshell membrane hydrolysates work additively to inhibit the severity of chronic inflammation.

Keywords: *Ageratum conyzoides*; anti-inflammatory; eggshell membrane hydrolysates; molecular docking; p38-MAPK.

Resumen

Contexto: El *Ageratum conyzoides* L. y la membrana de cáscara de huevo tienen potencial para ser utilizados como medicamentos. El uso independiente del extracto de *A. conyzoides* o de los hidrolizados de membrana de cáscara de huevo como medicina natural es ampliamente conocido, pero no se ha estudiado la mezcla de ambos como antiinflamatorio.

Objetivos: Evaluar los efectos antiinflamatorios *in vivo* e *in vitro* del extracto de *A. conyzoides* y de los hidrolizados de membrana de cáscara de huevo, independientemente y en combinación. Se realizaron pruebas *in silico* para identificar sustancias químicas que desempeñan un papel clave en las vías de señalización de la inflamación.

Métodos: Se evaluaron los efectos antiinflamatorios crónicos del extracto de *A. conyzoides* y de los hidrolizados de membrana de cáscara de huevo en ratas inducidas por gránulos de algodón, utilizando diclofenaco-Na como control. *In vitro*, los efectos antiinflamatorios se estudiaron mediante la desnaturalización de proteínas, la estabilidad de la membrana y la actividad antiproteasa. Además, se realizó un acoplamiento molecular de la vía de señalización p38-MAPK utilizando compuestos presentes en el extracto de *A. conyzoides* y en los hidrolizados de membrana de cáscara de huevo.

Resultados: El extracto de *A. conyzoides* y los hidrolizados de membrana de cáscara de huevo administrados por separado o en combinación pueden inhibir la formación de exudados y granulomas. Las simulaciones de acoplamiento molecular mostraron que los metabolitos del extracto y el hidrolizado interactúan con p38-MAPK. La nobiletina del extracto es el metabolito potencial que interactúa con el receptor p38-MAPK con una energía libre de unión y una constante de inhibición de -8,92 kcal/mol y 260,80 nM. Los aminoácidos de los hidrolizados mostraron interacciones más débiles en comparación con el compuesto del extracto.

Conclusiones: El extracto de *A. conyzoides* y los hidrolizados de membrana de cáscara de huevo actúan de forma aditiva para inhibir la gravedad de la inflamación crónica.

Palabras Clave: acoplamiento molecular; *Ageratum conyzoides*; anti-inflamatorio; hidrolizados de membrana de cáscara de huevo; p38-MAPK.

ARTICLE INFO
Received: January 24, 2024.
Accepted: May 10, 2024.
Available Online: May 21, 2024.

AUTHOR INFO
ORCID: 0000-0002-1486-8594 (SNV) 0000-0002-5145-5668 (TS)
0000-0003-3540-012X (EYS) 0000-0001-5217-2312 (IKA)

Abbreviations: ACE: *Ageratum conyzoides* extract; BBB: Blood-brain barrier; CAM: Complementary and alternative medicine; ESM: Eggshell membrane; ESMH: Eggshell membrane hydrolysates; HBA: Hydrogen bond acceptor; HBD: Hydrogen bond donor; IFN: Interferon; IL: Interleukin; NE: Neutrophil elastase; NET: Neutrophil extracellular traps; NL: Native ligand; p38-MAPK: p38-Mitogen-activated protein kinase; PR3: Proteinase 3; TNF-α: Tumor necrosis factor alpha.

INTRODUCTION

Currently, complementary and alternative medicine (CAM) is an alternative to conventional medicine. Ease of access to information regarding the effectiveness, safety, and contraindications of CAM therapy can help patients choose the right method (Sharma et al., 2016). Adult patients utilize CAM to treat pain (back pain, neck discomfort, joint pain, arthritis), headaches, allergies, skin problems, and gastrointestinal and cardiovascular disorders (Kemppainen et al., 2018). CAM treatments include herbal medicine, acupuncture, homeopathy, acupressure, aromatherapy, chiropractic, and naturopathy (Clarke et al., 2015). Even though it is categorized as CAM, the use of natural products has contributed to the development of new drugs. Natural products contain many chemical compounds that have biological activity and have the potential to be developed as new lead compounds and scaffolds (Yuan et al., 2016). The most widely used CAMs are natural products, such as *Ginkgo biloba*, chondroitin, garlic, flaxseed oil/pills, echinacea, fish oil/omega 3, glucosamine, ginseng, and mixtures of herbs (Wang et al., 2015).

Ageratum conyzoides L. (*Asteraceae*) has served as a medicinal remedy for generations. Ethnopharmacological studies revealed its utilization in treating wounds and skin disorders, reducing fever, preventing flu and coughs, asthma and dyspnea, leprosy, and arthrosis, and also addressing sexual dysfunction and infertility disorders (Kotta et al., 2020; Paul et al., 2022; Yadav et al., 2019). The compounds contained in *A. conyzoides* include 1,2-benzopyrone, quercetin, hyperoside, kaempferol, nobiletin, luteolin, apigenin, and eupalestin (Tambunan et al. 2017). Independent use of *A. conyzoides* extract and fractions showed anti-inflammatory effects. Research on the anti-inflammatory effects of *A. conyzoides* leaves and herbs using carrageenan induction shows that the extract is able to inhibit the formation of edema (Vigil de Mello et al., 2016; Vikasari et al., 2022). The administration of a hydroalcoholic extract of *A. conyzoides* leaves at doses of 250 and 500 mg/kg BW inhibited the proliferative phase of inflammation. The extract can prevent granuloma formation in animals caused by cotton pellets and formaldehyde. No abnormalities were observed in biochemical and hematological parameters during the 90-day safety assessment of the extract. There was no hepatotoxicity even though there was a 30.2% reduction in SGOT function at a dose of 500 mg/kg BW (Moura et al., 2005). *A. conyzoides* can be used independently or mixed with extracts or other substances. It has been combined with, for instance, extract from *Chromolaena odorata*, *Centella asiatica*, and honey. Mixing extracts from *A. conyzoides* and *C. odorata* at 10 mg/kg BW each possesses antioxidant properties and reduces blood glucose and cholesterol levels (Uhegbu et al., 2016). The gel containing a combination of extracts of *A. conyzoides*, *C. asiatica,* and astaxanthin can speed healing in open wounds (Sukmawan et al., 2021). The usage of honey and *A. conyzoides* extract (ACE) together can strengthen the gastrointestinal mucosal cells' resistance to ethanol-HCl mixture-induced irritation (Fathihah et al., 2005).

Eggshells are a waste product with potential applications in medicine. The exterior layer of the eggshell, known as the eggshell membrane (ESM), is constructed out of fibrous fibers. The following substances are known to be present in ESM: hyaluronic acid, defensin, chondroitin sulfate, fibronectin, keratin, histones, and osteopontin (Shi et al., 2021). ESM can be used as a medication as ESM powder or hydrolysates (ESMH). Forms of ESM and ESMH used independently are employed in medicine for a wide range of circumstances, such as cardiovascular disease (Moreno-Fernández et al., 2020), gastrointestinal disorders (Jia et al., 2017), joint health (Wedekind et al., 2017), anti-microbials (Li et al., 2019), skin and wound healing (Choi et al., 2021; Sim et al., 2023; Vuong et al., 2018). Both preclinical and clinical evidence support the use of ESMH and ESM as anti-inflammatories. Preclinical *in vitro* experiments using lipopolysaccharide-induced RAW264.7 cell revealed that ESMH is anti-collagenase, elastase active, and inhibits pro-inflammatory cytokines (Lee et al., 2017; Yoo et al., 2014). ESM is able to reduce the pro-inflammatory cytokines IL-1β, TNF-α, MCP-1, MIP-1α and β, RANTES, and VEGF after being used for seven days on test animals (Ruff and DeVore, 2014). Evidence from human clinical trials indicates that ESM/ESMH can reduce stiffness and cartilage turnover (Ruff et al., 2018), as well as decrease pain (Kiers and Bult, 2021), and enhance joint function in people with osteoarthritis (Cánovas et al., 2022). It is still uncommon to find ESM mixed with extracts, and its use is still restricted when evaluating its antibacterial properties. Antioxidant and antibacterial benefits of ESM are enhanced when used in conjunction with extracts of *Thymus vulgaris* and *Origanum vulgare* (Webb et al., 2022), as well as when integrated with olive leaf extract (Bayraktar et al., 2021).

One of the challenges in developing natural products into modern medicines is the identification of key chemical compounds and their corresponding targets of action (Thomford et al., 2018). Computational approaches to receptor-ligand interactions are required to provide insight into the binding mechanism, affinity, and possible therapeutic impact of natural product molecules on protein targets (Tian et al., 2015). The *in silico* approach can be used to understand cell communication through the signal transduction process (Lindvall et al., 2003). A class of kinases known as mitogen-activated protein kinase (MAPK) is engaged in both intracellular and extracellular signal transduction pathways. The MAPK pathway is divided into three sections: extracellular signal-regulated protein kinase (ERK), c-JUN N-terminal kinase/stress-activated protein kinase (JNK/SAPK), and p-38 kinase (p38-MAPK) (Kim and Choi, 2015). However, no *in silico* studies have been found regarding the *A. conyzoides* and ESMH compounds in the MAPK pathway, especially p38-MAPK.

The use of a combination or mixture of natural products has several advantages, including reducing the effective dose for single use, providing a synergistic effect on several work targets, and reducing the risk of resistance (Sun et al., 2022).The use of a combination of natural products (plants or botanical preparations) is expected to reduce adverse effects and provide advantages through additive pharmacokinetic and pharmacodynamic interactions (Caesar and Cech, 2019). As mentioned above, the combined use of ACE and/or ESMH with other natural products is very limited. *ACE* and ESM/ESMH each have anti-inflammatory properties, but no research has been found on the combination of the two as an anti-inflammatory. Anti-inflammatory drugs are often used in various diseases, for example, cardiovascular disorders, arthritis, asthma, diabetes, and central nervous system disorders (Laveti et al., 2013). Therefore, it is necessary to study the potential of a mixture of babadotan and ESM/ESMH as an anti-inflammatory. Thus, this study aims to examine the anti-inflammatory effects of an ethanol extract of *A. conyzoides* leaves combined with ESMH in an animal model of sub-acute inflammation induced by cotton pellets. The combined usage of ACE and ESMH are expected to provide better effects compared to their individual application, while additionally targeting multiple pathways. The next step of this study was a computational approach to receptor-ligand interactions between *A. conyzoides* and ESMH compounds on p38-MAPK targets. By bridging the gap between traditional medicinal knowledge and modern computational methodologies, this study contributes to the ongoing quest for effective, natural-based treatments for inflammation, offering a foundation for further experimental validation and drug discovery efforts.

MATERIAL AND METHODS

Materials and reagents

The *Ageratum conyzoides* leaves for this study were collected from Pancoran village, Bondowoso, East Java (GPS 7° 57′ 35.78″S 113° 48′ 14.44″ E). Determination of the test material was conducted at the School of Life Sciences and Technology, Bandung Institute of Technology, with specimen number 118/IT1.C11.2/TA.00/2023.

The eggshell membrane (ESM) was obtained from the food industry in Bandung, West Java (GPS 6° 53' 55.55"S 107° 36' 28.52"E). Evaluation of the test material was conducted at the School of Life Sciences and Technology, Bandung Institute of Technology. The reagents used were bovine serum albumin (Sigma Aldrich®), phosphate buffer pH 6.4 (Merck®), and sodium diclofenac (Kimia Farma).

Preparation of *Ageratum conyzoides* extract and eggshell membrane hydrolysates

After being collected, the *A. conyzoides* leaves and ESM were cleaned and allowed to dry. The leaves and ESM shrunk in size after drying. The *A. conyzoides* leaf extract was prepared under reflux using 50% ethanol as a solvent. Extraction was performed three times. The resultant liquid extract was concentrated using a rotary evaporator to obtain a concentrated extract with a constant weight (Vikasari et al., 2022). The eggshell membrane was dissolved in 40% ethanol, and 2 N NaOH was used to obtain a pH of 12. After that, the mixture was agitated at 250 rpm for two hours at 60°C. After filtration, acetic acid was added up to neutral pH. The filtrates were then dried until the weight remained constant (Vikasari et al., 2024).

Chronic anti-inflammatory using cotton pellet induction

Chronic anti-inflammatory assessment was conducted using cotton pellet induction. The assessment was conducted according to institutional ethical approval 8025/KEP-UNJANI/I/2021. The Wistar rats (male, weight 165-190 g) were procured from the Animal Laboratory of the Centre for Biosciences and Biogenetics, Institut Teknologi Bandung. The animals were adapted for one week and 18 hours before the experiment, the animals were fasted and still given water *ad libitum*. Animals were placed in a room with a 12:12-h light:dark cycle and at a room temperature of 25-28°C.

This experimental research was a randomized block design with multiple independent variables. The research was divided into a control group and an experimental group. The doses of *A. conyzoides* extract (ACE) and eggshell membrane hydrolysates (ESMH) in the experimental group were obtained from previous research. Acute anti-inflammatory tests in animals induced by carrageenan showed ESMH at dosages of 22.5, 45, and 90 mg/kg BW (Vikasari et al., 2024) and ACE at dosages of 45 and 90 mg/kg BW (Vikasari et al., 2022) were able to inhibit inflammation and equivalent to the comparison of diclofenac sodium.

The chronic anti-inflammatory experiment was conducted on eight groups, namely (1) control, (2) diclofenac sodium 2.25 mg/kg BW, (3) ESMH at 22.5 mg/kg BW, (4) ACE at 45 mg/kg BW, (5) Mixture C1 (ACE 45 mg/kg BW and ESMH 22.5 mg/kg BW), (6) Mixture C2 (ACE 11.25 mg/kg BW and ESMH 16.875 mg/kg BW), (7) Mixture C3 (ACE 22.5 mg/kg BW and ESMH 11.25 mg/kg BW), and (8) Mixture C4 (ACE 33.75 mg/kg BW and ESMH 5.625 mg/kg BW).

Aseptic procedures were followed during the experiment, and the cotton pellets (±50 mg) were autoclave-sterilized for 30 minutes at 120°C. Ketamine (0.5 mL/kg BW i.m.) was used to anesthetize the animals. Then, the fur on the animal's back was cleaned and the animal was induced with sterile cotton pellets via s.c. After being induced, each test animal received preparations according to the group (p.o.) for seven days. On the 8th day, the animals were checked for hematological profiles using a hematology analyzer (Melet Schloessing ®). Then, they were anesthetized and dissected to remove cotton pellets and granuloma tissue, and the wet pellets obtained were weighed. After that, the wet pellets were dried for 24 hours at a temperature of ±60°C, and the dry pellets were weighed. Then, the weight of the exudate and granuloma was calculated, as well as the percent inhibition of exudate and granuloma, using equations [1] and [2] (Rafiyan et al., 2023).

$$\text{Exudate inhibition (\%)} = \left(1 - \frac{\text{Exudate in treated group}}{\text{Exudate in control}}\right) \times 100\% \quad [1]$$

$$\text{Granuloma inhibition (\%)} = \left(1 - \frac{\text{Granuloma in treated group}}{\text{Granuloma in control}}\right) \times 100\% \quad [2]$$

In vitro anti-inflammatory assay

In vitro anti-inflammatory assays were conducted to assess protein denaturation inhibition and anti-proteinase activity.

Protein denaturation inhibition

A total of 20 µL of the sample (water/diclofenac-Na/ACE/ESMH) was mixed with 200 µL 1% bovine serum albumin (BSA) and 4.78 mL of phosphate buffer saline pH 6.4. The mixture was incubated at 37°C for 15 minutes. After that, it was heated for five minutes at 70°C. After cooling under running water, the absorbance was measured at 660 nm in spectrophotometer UV-Vis (Shimadzu 1800, Shimadzu, Japan). The tests were performed in triplicate. The percentage inhibition of protein denaturation was then calculated using equation [3]. From the data obtained, the IC_{50} value was determined using linear regression (Gunathilake et al., 2018; Kamala Lakshmi and Valarmathi, 2020).

$$\text{Protein denaturation inhibition (\%)} = \left(1 - \frac{\text{Absorbance in treated group}}{\text{Absorbance in control}}\right) \times 100\% \quad [3]$$

Anti-proteinase activity

A total of 1 mL of the sample (water/diclofenac-Na/ACE/ESMH) was combined with 2 mL of 3% trypsin and 1 mL of 20 mM Tris HCl buffer (pH 7.4). The mixture was then incubated for five minutes at 37°C. After that, 1 mL of 0.8% casein was added and incubated for another 20 minutes. To stop the reaction, 2 mL of 70% perchloric acid was added. The mixture was then centrifuged for ten minutes at 3000 rpm. The absorbance was then measured at 210 nm in spectrophotometer UV-Vis (Shimadzu 1800, Shimadzu, Japan). The tests were performed in triplicate, and the percentage of anti-proteinase activity was calculated using equation [4]. From the data obtained, the IC_{50} value was determined using linear regression (Gunathilake et al., 2018).

$$\text{Antiproteinase activity (\%)} = \left(1 - \frac{\text{Absorbance in treated group}}{\text{Absorbance in control}}\right) \times 100\% \quad [4]$$

Membrane stabilization assay

The membrane stabilization test was performed using heat induction and hypotonic fluid (Kamala Lakshmi and Valarmathi, 2020). The blood was obtained from the Indonesian Red Cross in Bandung, Indonesia. The blood was then centrifuged at 3000 rpm for 10 minutes before being rinsed three times with 0.9% NaCl. The erythrocyte suspension obtained was reconstituted into 10% with 0.9% NaCl.

Heat-induced hemolysis

A total of 1 mL of the sample (water/diclofenac-Na/ACE/ESMH) was mixed with 1 mL of 10% erythrocyte suspension. The mixture was incubated for 30 minutes at 56°C in a water bath. Running water was used to cool the material after incubation. The mixture was centrifuged for five minutes at 2500 rpm, and the absorbance was determined at a wavelength of 560 nm in spectrophotometer UV-Vis (Shimadzu 1800, Shimadzu, Japan). The tests were performed in triplicate, and the percentage of hemolysis inhibition

was calculated using equation [5]. From the data obtained, the IC_{50} value was determined using linear regression (Gunathilake et al., 2018; Kamala Lakshmi and Valarmathi, 2020).

$$\text{Hemolysis inhibition (\%)} = \left(1 - \frac{\text{Absorbance in treated group}}{\text{Absorbance in control}}\right) \times 100\% \quad [5]$$

Hypotonicity induced hemolysis

A total of 1 mL of the sample (water/diclofenac-Na/ACE/ESMH) was mixed with 1 mL of 10% erythrocyte suspension and 2 mL of hyposaline. The mixture was incubated for 30 minutes at 37°C in a water bath. After that, the mixture was centrifuged for 20 minutes at 3000 rpm, and the supernatant was measured at a wavelength of 560 nm in spectrophotometer UV-Vis (Shimadzu 1800, Shimadzu, Japan). The tests were performed in triplicate, and the percentage of hemolysis inhibition was calculated (equation [6]). From the data obtained, the IC_{50} value was determined using linear regression (Kamala Lakshmi and Valarmathi, 2020).

$$\text{Hemolysis inhibition (\%)} = \left(1 - \frac{\text{OD in treated group}}{\text{OD in control}}\right) \times 100\% \quad [6]$$

In silico analysis of drug-like properties, pharmacokinetic profile and toxicity prediction, and molecular docking simulation

Analysis of drug-like properties, pharmacokinetic profile, and toxicity prediction

Analysis of drug-like properties of compounds in ACE and ESMH was carried out based on Lipinski's rule of five, which states that a compound has properties similar to drugs if the molecular weight (MW) of the compound is less than 500 Daltons, the partition coefficient value log P is less than 5, the number of hydrogen bond donors (HBD) is less than 5, and the number of hydrogen bond acceptors (HBA) is less than 10. This analysis is carried out mainly for compounds that are used orally (Lipinski, 2004). Prediction of the compound's pharmacokinetic profile was evaluated through absorption, distribution, metabolism, and excretion (ADME), and toxicity predictions were also carried out. The compound from ACE and ESMH were obtained from previous research data (Jain and Anal, 2017; Tambunan et al., 2017), and the structure was created in 3D SDF or MOL2 format (Asnawi et al., 2023). The existing 3D SDF ligand structure was converted into canonical SMILES (simple molecular-input line-entry system) format. The SwissADME (http://www.swissadme.ch) was employed to conduct an analysis of drug similarity properties. pkCSM (https://biosig.unimelb.edu.au/pkcsm) was utilized to predict the ADMET profile (absorption, distribution, metabolism, and excretion), while ProTox-3.0 (https://comptox.charite.de/protox3) was employed to predict toxicity.

Molecular docking simulation

Molecular docking simulation of ACE and ESMH compounds from previous research data (Jain and Anal, 2017; Tambunan et al., 2017) was carried out against the inflammatory pathway target (p38-MAPK) using Autodock Wizard in PyRx. The structure compound was created in 3D SDF or MOL2 format, which was then converted to PDBQT format using PyRx (Asnawi et al., 2023). Target proteins p38-MAPK (PDB ID 3NEW) were obtained from the RCSB Protein Data Bank (Schnieders et al., 2012). Structural issues were checked and corrected using molecular visualization tools using Discovery Studio Visualizer. The docking grid box that encompassed the active site of each target protein was defined, thoroughly covering the binding pocket for accurate ligand docking. Lamarckian genetic algorithm (GA) was chosen as the docking algorithm (Fuhrmann et al., 2010). Autodock simulations were run for each ligand-protein pair, allowing the ligand to explore the binding site and find energetically favorable conformations. The progress of the simulations was monitored, with an analysis of cluster structures used to evaluate both convergence and ligand flexibility. Docking results were validated by comparing them with known binding modes of reference ligands or experimental data. Analysis was performed to identify ligands with the most favorable binding affinities and interactions across all target proteins.

Statistical analysis

All of the information on chronic anti-inflammatory assessment is displayed in the form of the mean, along with the standard error of the mean. Statistical analysis with one way analysis of variance (ANOVA) followed by Fisher's LSD post hoc. The $p<0.05$ indicates significance. *In vitro* anti-inflammatory data are presented in the form of single data. The IC_{50} value was obtained from linear regression analysis. All statistical analysis was done using GraphPad Prism 8.0.2. Data analysis of drug-like properties and ADMET prediction is presented in tabular form, while plots and tables were generated to present the docking results comprehensively.

RESULTS

Chronic anti-inflammatory using cotton pellet induction

In inflammation, endothelial cells will experience vasodilation, causing an increase in blood volume in

the inflamed area. Congestion will also increase hydrostatic pressure so that plasma fluid is pushed out of the tissue (transudate), causing edema in the tissue (Serhan et al., 2019). In chronic inflammation, macrophages will continue to work, especially removing food waste and dead neutrophils, and often form characteristic formations around pathogens or foreign objects that cause inflammation, called granulomas (Ganesan et al., 2022). The weight of exudate and granuloma in the chronic inflammation assay is observed in Table 1. An increase in the weight of exudate and granuloma indicates chronic inflammation. When compared to the control group, the administration of ACE and ESMH separately and their mixture was able to suppress the formation of exudate and granulomas ($p<0.05$). On separate use, ESMH provides an inhibitory effect on exudate and granuloma formation 1.75 times better than the separate use of ACE. The four mixtures of ACE and ESMH provide anti-inflammatory effects, with the order from highest to lowest effects being C1>C4>C3>C2.

Numerous blood cells and proteins, as well as those found in blood vessels and connective tissue, are involved in the inflammatory process. Some of the cells involved include neutrophils, lymphocytes, basophils, mast cells, monocytes, macrophages, and platelets (Pober and Sessa, 2015). At the end of the anti-inflammatory assessment, the administration of diclofenac-Na decreased all of the hematological parameters when compared to the controls. Administration of ACE or ESMH separately may cause a decrease in leucocytes, lymphocytes, mid-sized cells, and granulocyte counts when compared with the control group. Furthermore, ACE or ESMH can increase platelet counts compared to the control group. The mixtures of ACE and ESMH (C1, C2, and C3) almost give a similar effect to diclofenac. They could decrease all of the hematological parameters when compared to the controls (Table 2).

In vitro anti-inflammation assay

In vitro studies have been conducted to examine the mechanism of the anti-inflammatory effect, including the ability to inhibit protease inhibitors, membrane stability, and protein denaturation (Fig. 1). The calculation of the IC_{50} value is based on the percentage of inhibition. Fig. 1A reveals that ACE and ESMH concentrations of 20-100 µg/mL can inhibit protein denaturation by 25-70%, with an IC_{50} value <100 µg/mL. This suggests a capacity to inhibit protein denaturation, although less potent than diclofenac-Na. The antiprotease activity of ACE (40-180 µg/mL) and ESMH (40-320 µg/mL) within a 15-70% range is shown in Fig. 1B. Although both ACE and ESMH showed moderate antiprotease activity, ACE showed a greater antiprotease activity than ESMH. Fig.1C and Fig. 1D demonstrate how ACE and ESMH can stabilize membranes; Fig. 1C shows heat-induced, whereas Fig. 1D explains hypotonic-induced. In Fig. 1C, ACE and ESMH exhibit at doses ranging from 2.5 to 40 µg/mL were able to stabilize heat-induced membranes by 25-60%. According to Fig. 1D, heat-induced membranes could be stabilized in the 35-70% range by using ACE and ESMH at concentrations of 4-80 µg/mL.

Table 1. Effects of *A. conyzoides*, eggshell membrane hydrolysates, and their combination on cotton pellet-induced granuloma in rats.

Group	Exudate weight (mg)	Exudate inhibition (%)	Granuloma weight (mg)	Granuloma inhibition (%)
Control	331.36 ± 50.58	-	277.36 ± 47.44	-
Diclofenac-Na	153.14 ± 17.92*	53.78	102.34 ± 14.70*	63.10
ACE	212.10 ± 8.60*	35.99	163.70 ± 10.77*	40.98
ESMH	128.68 ± 18.23*	61.17	79.08 ± 16.47*	71.49
Mixture C1	157.84 ± 37.06*	52.37	107.04 ± 41.19*	61.41
Mixture C2	248.98 ± 27.07*	24.86	203.78 ± 27.97*	26.53
Mixture C3	231.72 ± 8.29*	30.07	182.52 ± 8.97*	34.19
Mixture C4	170.56 ± 14.52*	48.53	120.56 ± 19.99*	56.53

Data are expressed as mean ± SEM or SD (n = 5). Statistical analysis using ANOVA followed by Fisher's LSD post hoc. *p<0.05 statistically significant difference compared to the control group.

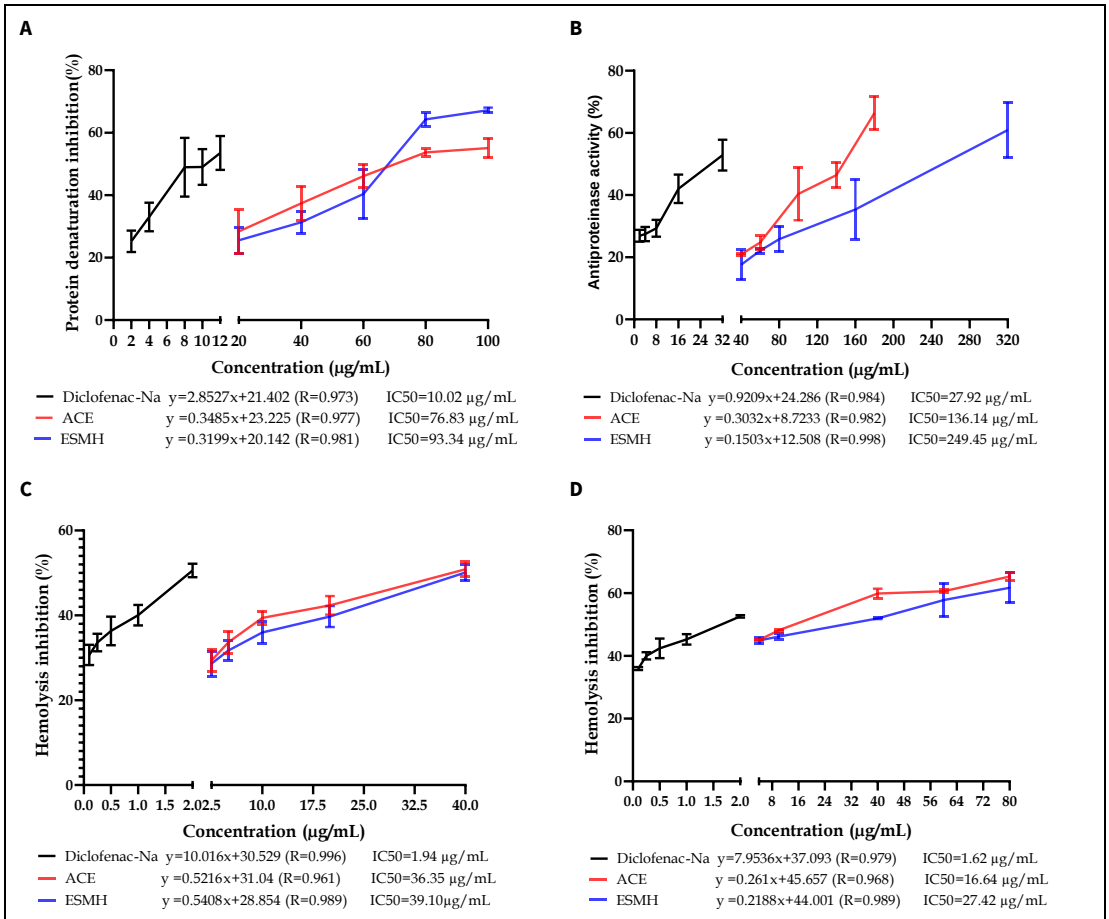

Figure 1. *In vitro* anti-inflammatory effect.

(A) Effect on protein denaturation; **(B)** Effect on anti-proteinase activity; **(C)** Effect on heat-induced hemolysis; **(D)** Effect on hypotonic-induced hemolysis. Data are expressed as mean ± SEM of the triplicate test.

In silico analysis of drug-like properties, pharmacokinetic profile and toxicity prediction, and molecular docking simulation

An orally active drug-like compound should not have more than one violation of the following criteria as stated by Lipinski's rule (Lipinski, 2004). An assessment of drug similarity was performed using the SwissADME web-based tool. SwissADME allows beneficial access to a database of robust and rapid predictive models for physicochemical properties, pharmacokinetics, drug-likeness, and medicinal chemistry friendliness (Daina et al., 2017). The results of the drug similarity analysis (Table 3) show that all the amino acids in ESMH and several compound contents in ACE (monohydroxy-penta-methoxy-flavone, nobiletin, eupalestin, luteolin, kaempferol-7-O-rhamnopyranoside, and apigenin) meet the requirements Lipinski's rule. Quercetin-3-glucoside, hyperoside, astragaline, and luteolin-7-O-glucuronide do not meet the requirements of HBA and HBD parameters, whereas quercetin-3-O-rutinoside does not meet the requirements for HBA, HBD, and MW parameters. The compound has a value greater than required: BM > 500 daltons, HBA > 10, and HBD > 5. Based on the results of this analysis, it can be stated that all the amino acids in ESMH and several compounds in ACE (monohydroxy-penta-methoxy-flavone, nobiletin, eupalestin, luteolin, kaempferol-7-O-rhamnopyranoside, and apigenin) have similar properties to drugs.

pkCSM is a computational approach that can be used to predict the pharmacokinetic profile of a small-molecule and its toxicity properties using graph-based signatures. Pharmacokinetic parameters include absorption, distribution, metabolism, and excretion (Pires et al., 2015).

Absorption is predicted by calculating the Caco2 permeability, intestinal absorption, and skin permeability. Caco2 permeability and intestinal absorption are assessed during the oral administration of the drug, while skin permeability is evaluated in the case of topical/transdermal administration. The Caco-2 permeability coefficient value is utilized to predict the absorption of orally administered pharmaceuticals using an *in vitro* model of the human intestinal mucosa (Adianingsih et al., 2022; AL Azzam, 2023).

Table 2. Effect of *A conyzoides*, eggshell membrane hydrolysates and their combination on hematological profile on cotton pellet induced granuloma in rats.

Groups	WBC	LYM	MID	GRA	RBC	HGB	PLT
Control	47.96 ± 2.71	23.29 ± 2.49	10.36 ± 0.94	14.55 ± 3.00	8.02 ± 0.74	125.60 ± 7.83	567.40 ± 73.44
Diclofenac-Na	35.11 ± 2.95	14.93 ± 3.67*	6.37 ± 1.94	7.75 ± 1.22	7.83 ± 1.07	119.40 ± 19.72	454.00 ± 28.42
ACE	41.18 ± 9.91	21.89 ± 5.79	8.38 ± 1.85	10.91 ± 3.11	8.07 ± 0.96	122.60 ± 16.50	673.60 ± 46.01
ESMH	35.83 ± 2.76	20.21 ± 2.89	7.69 ± 0.48	7.94 ± 0.79	8.48 ± 0.26	127.60 ± 5.73	956.20 ± 85.07
Mixture C1	45.40 ± 3.99	22.57 ± 2.24	9.48 ± 1.07	14.21 ± 1.50	7.64 ± 0.39	119.40 ± 6.95	496.20 ± 97.10
Mixture C2	44.18 ± 4.61	23.69 ± 1.71	8.11 ± 0.97	12.30 ± 2.19	7.57 ± 0.41	118.60 ± 10.19	446.00 ± 30.43*
Mixture C3	42.84 ± 15.77	23.38 ± 9.20	7.82 ± 2.03	11.59 ± 4.95	6.99 ± 1.72*	114.60 ± 25.10	447.40 ± 92.95*
Mixture C4	44.25 ± 4.21	23.47 ± 3.67	9.14 ± 1.30	12.34 ± 1.42	8.03 ± 0.59	124.60 ± 7.64	629.40 ± 73.37

Data are expressed as mean ± SEM (n = 5). Statistical analysis using ANOVA followed by Fisher's LSD post hoc. *p<0.05 statistically significant difference compared to the control group. WBC: White blood cell; LYM: Lymphocyte; MID: Mid-sized cell; GRA: Granulocyte; RBC: Red blood cell; HGB: Hemoglobin; PLT: Platelet.

A drug tends to be easily absorbed in the gastrointestinal tract if the Caco-2 permeability coefficient (log Papp) value is more than 0.90 cm/s and intestinal absorption is high. Meanwhile, drugs are more effective given topically/transdermally if the skin permeability value (log Kp) is more than -2.5 cm/hour (Adianingsih et al., 2022; AL Azzam, 2023). The findings of the analysis, as presented in Table 4, indicate that diclofenac-sodium, several amino acids in ESMH (glycine, alanine, methionine, and proline), and several compounds in ACE (nobiletin, eupalestin, luteolin, quercetin-3-O-rutinoside, and apigenin) present good intestinal absorption and/or Caco-2 permeability coefficient. All amino acids in ESMH and compounds in ACE show skin permeability (log Kp) of more than -2.5 cm/hour. They are expected to have high skin penetration.

Predictions of distribution are derived through analysis of the blood-brain barrier (BBB) permeability and VDss values. VDss is the theoretical volume of the total dose of the drug, which must be distributed evenly to provide the same concentration as in blood plasma. Distribution is considered high if VDss > 0.45. A drug's capacity to traverse the BBB is crucial for minimizing adverse effects and toxicity, as well as enhancing the pharmacological activity of the drug. BBB was measured experimentally. A logBB value greater than 0.3 indicates that a compound can easily traverse the blood-brain barrier (Adianingsih et al., 2022; AL Azzam, 2023). According to the results presented in Table 4, multiple compounds in ACE (quercetin-3-glucoside, hyperoside, astragaline, kaempferol-7-O-rhamnopyranoside, luteolin, quercetin-3-O-rutinoside, luteolin-7-O-glucuronide, and apigenin) distributed relatively fairly throughout the plasma. The amino acids in ESMH (except valine) and all compounds in ACE are unable to penetrate the BBB. Following distribution, the drug is metabolized. CYP450 is involved in the liver and intestines' metabolism of drugs and xenobiotics (Adianingsih et al., 2022; AL Azzam, 2023).

According to the analysis results (Table 4), several substances in ACE (monohydroxy-penta-methoxy-flavone, nobiletin, and eupalestin) influence metabolism by inhibiting CYP450. The excretion profile is observed on the total clearance and OCT2 (organic cation transporter 2) substrates. Drug clearance is calculated as the sum of hepatic clearance (metabolism in the liver and bile ducts) and renal clearance. Renal OCT2 substrate is a reuptake transporter that has an important role in the disposition and clearance of drugs and renal endogenous compounds (Adianingsih et al., 2022; AL Azzam, 2023). According to the data presented in Table 4, a number of the amino acids in ESMH (trypthophan, proline, and histidine) and the compounds in ACE (monohydroxy-penta-methoxy-flavone, nobiletin, and eupalestin) have a total clearance greater than 0.5. Furthermore, none of the compounds in ACE are OCT2 substrates.

ProTox-3.0 is a web server dedicated to the predictive toxicity of small molecules. This computational approach predicts various potential toxicities in organs (hepatotoxic, carcinogenic, mutagenic, and cytotoxic), the LD_{50} value, and toxicity class. LD_{50} is the dose (in mg/kg BW) that can cause death in 50% of test animals within a certain time period. Class toxicity predictions show that the smaller the class indicated, the greater the predicted toxicity, and vice versa. The larger the class indicated, the safer the compound (Banerjee et al., 2018). The analysis results (Table 5) show that the compounds predicted to be hepatotoxic are eupalestin and diclofenac. The compounds in ACE that are predicted to be carcinogenic are kaempferol-7-O-rhamnopyranoside, luteolin, and luteolin-7-O-glucuronide. Compounds predicted to have mutagenicity are luteolin, lysine, and cysteine.

Table 3. Analysis of drug-like properties of *Ageratum conyzoides* metabolite and eggshell membrane hydrolysates using SwissADME.

No.	Metabolite*	Formula	MW	HBA	HBD	TPSA	Log P	Violations
	Native ligand Compound 10	$C_{20}H_{23}N_7O_7$	473.44	8	7	219.84	-0.93	2
	Diclofenac	$C_{14}H_{11}Cl_2NO_2$	296.15	2	2	49.33	0.17	0
	***Ageratum conyzoides* extract**							
1.	Quercetin-3-glucoside	$C_{21}H_{20}O_{12}$	464.38	12	8	210.51	-0.48	2
2.	Hyperoside	$C_{21}H_{20}O_{12}$	464.38	12	8	10.51	-0.38	2
3.	Monohydroxy-penta-methoxy-flavone	$C_{20}H_{20}O_7$	372.37	7	0	76.36	3.02	0
4.	Astragaline / kaempferol 3-O-glucoside	$C_{21}H_{20}O_{11}$	448.34	11	7	190.28	-0.09	2
5.	Nobiletin	$C_{21}H_{22}O_8$	402.39	8	0	85.59	3.02	0
6.	Kaempferol-7-O-rhamnopyranoside	$C_{21}H_{20}O_{10}$	432.38	10	6	170.05	0.04	1
7.	Eupalestin	$C_{21}H_{20}O_9$	416.38	9	0	94.82	0.14	0
8.	Luteolin	$C_{15}H_{10}O_6$	286.24	6	4	111.13	0.09	0
9.	Quercetin-3-O-rutinoside		610.52	16	10	240.90	-1.69	3
10.	Luteolin-7-O-glucuronide	$C_{21}H_{18}O_{12}$	462.36	12	7	207.35	-0.06	2
11.	Apigenin	$C_{15}H_{10}O_5$	370.24	5	3	90.90	2.11	0
	Eggshell membrane hydrolysate							
12.	Glycine (Gly)	$C_2H_5NO_2$	75.07	3	2	63.32	-1.69	0
13.	Alanine (Ala)	$C_3H_7NO_2$	89.09	3	2	63.32	-1.46	0
14.	Arginine (Arg)	$C_6H_{14}N_4O_2$	174.20	4	4	127.72	-2.08	0
15.	Glutamic acid (Glu)	$C_5H_9NO_4$	147.13	5	3	100.62	-1.68	0
16.	Aspartic acid (Asp)	$C_4H_7NO_4$	133.1	5	3	100.62	-2.05	0
17.	Phenylalanine (Phe)	$C_9H_{11}NO_2$	165.19	3	2	63.32	-0.01	0
18.	Histidine (His)	$C_6H_9N_3O_2$	155.15	4	3	92.00	-1.54	0
19.	Isoleucine (Ile)	$C_6H_{13}NO_2$	131.17	3	2	63.32	-0.40	0
20.	Leucine (Leu)	$C_6H_{13}NO_2$	131.17	3	2	63.32	-0.38	0
21.	Lysine (Lys)	$C_6H_{14}N_2O_2$	146.19	4	3	89.34	-1.19	0
22.	Methionine (Met)	$C_5H_{11}NO_2S$	149.21	3	2	88.62	-0.58	0
23.	Proline (Pro)	$C_5H_9NO_2$	115.13	3	2	49.33	-0.92	0
24.	Serine (Ser)	$C_3H_7NO_3$	105.09	4	3	83.55	-1.97	0
25.	Cysteine (Cys)	$C_3H_7NO_2S$	121.16	3	2	102.12	-1.31	0
26.	Threonine (Thr)	$C_4H_9NO_3$	119.12	4	3	83.55	-1.67	0
27.	Tyrosine (Tyr)	$C_9H_{11}NO_3$	181.19	4	3	83.55	-0.49	0
28.	Tryptophan (Trp)	$C_{11}H_{12}N_2O_2$	204.23	3	3	79.11	0.17	0
29.	Valine (Val)	$C_5H_{11}NO_2$	117.15	3	2	63.32	-0.78	0

MW: Molecular weight; HBA: Hydrogen bond acceptors; HBD: Hydrogen bond donors; TPSA: Topological polar surface area; P: Partition coefficient. *The characterization data of these metabolites were extracted from Jain and Anal (2017) and Tambunan et al. (2017) and analyzed by mean of http://www.swissadme.ch/

There are no amino acids in ESMH and no cytotoxic compounds in ACE. LD_{50} values for all amino acids in ESMH and compounds in ACE are higher than the value of diclofenac. In the same pattern as the predicted toxicity class, all ACE compounds and ESMH amino acids (except for serine) exhibit a toxicity class equivalent to or safer than diclofenac.

Molecular docking simulation

Molecular docking, a computational technique, allows for the *in silico* exploration of ligand-protein

Table 4. The pharmacokinetic profile prediction of *Ageratum conyzoides* metabolite and eggshell membrane hydrolysates using pkCSM.

No.	Metabolites	Absorption			Distribution		Metabolism			Excretion	
		Caco2 permeability (log Papp in 10-6 cm/s)	Intestinal absorption (%)	Skin permeability (log Kp)	VDss (human) (log L/kg)	BBB permeability (log BB)	CYP1A2 inhibitor	CYP2C19 inhibitor	CYP3A4 inhibitor	Total clearance (log mL/min/kg)	Renal OCT2 substrate
	Native ligand Compound 10	-1.150	8.262	-2.735	-1.209	-2.462	No	No	No	0.153	No
	Diclofenac	1.379	91.923	-2.724	-1.605	0.236	No	No	No	0.291	no
	***Ageratum conyzoides* extract**										
1.	Quercetin-3-glucoside	0.336	42.972	-2.735	1.423	-1.491	No	No	No	0.215	No
2.	Hyperoside	0.242	47.999	-2.735	1.846	-1.688	no	no	no	0.394	no
3.	Monohydroxy-penta-methoxy-flavone	0.327	100.000	-2.746	-0.028	-1.113	no	no	yes	0.648	no
4.	Astragaline / Kaempferol 3-O-glucoside	0.306	48.052	-2.735	1.444	-1.514	no	no	no	0.462	no
5.	Nobiletin	1.306	98.921	-2.715	-0.281	-1.254	yes	yes	yes	0.789	no
6.	Kaempferol-7-O-rhamnopyranoside	0.276	54.691	-2.735	1.167	-1.391	no	no	no	0.443	no
7.	Eupalestin	1.310	100.000	-2.739	-0.299	-1.423	Yes	Yes	yes	0.615	no
8.	Luteolin	0.096	81.130	-2.735	1.153	-0.907	yes	no	no	0.495	no
9.	Quercetin-3-O-rutinoside	0.949	23.446	-2.735	1.663	-1.896	no	no	no	-0.369	no
10.	Luteolin-7-O-glucuronide	-0.891	15.201	-2.735	0.864	-1.478	no	no	no	0.519	no
11.	Apigenin	1.007	93.250	-2.735	0.822	-0.734	yes	yes	no	0.566	no
	Eggshell membrane hydrolysate										
12.	Glycine (Gly)	0.459	80.995	-2.738	-0.532	-0.428	no	no	no	0.475	no
13.	Alanine (Ala)	0.466	81.091	-2.738	-0.534	-0.412	no	no	no	0.370	no
14.	Arginine (Arg)	-0.472	34.522	-2.735	-0.002	-0.704	no	no	no	0.159	no
15.	Glutamic acid (Glu)	-0.487	28.979	-2.735	-0.291	-0.692	no	no	no	0.205	no
16.	Aspartic acid (Asp)	-0.498	17.945	-2.735	-0.428	-0.707	No	No	No	0.145	No
17.	Phenylalanine (Phe)	0.620	76.210	-2.734	-0.326	-0.271	No	No	No	0.452	No
18.	Histidine (His)	-0.417	50.754	-2.735	-0.185	-0.910	No	No	No	0.668	No
19.	Isoleucine (Ile)	0.589	77.913	-2.737	-0.554	-0.325	No	No	No	0.329	No
20.	Leucine (Leu)	0.597	74.448	-2.736	-0.553	-0.310	no	no	no	0.203	no
21.	Lysine (Lys)	0.737	62.673	-2.735	-0.511	-0.518	no	no	no	0.500	no
22.	Methionine (Met)	0.641	81.604	-2.737	-0.560	-0.326	no	no	no	0.547	no
23.	Proline (Pro)	1.116	87.223	-2.735	-0.356	-0.310	no	no	no	0.632	no
24.	Serine (Ser)	0.414	68.865	-2.736	-0.461	-0.709	no	no	no	0.398	no
25.	Cysteine (Cys)	0.386	74.907	-2.737	-0.486	-0.398	no	no	no	0.530	no
26.	Threonine (Thr)	0.448	68.961	-2.736	-0.464	-0.731	no	no	no	0.342	no
27.	Tyrosine (Tyr)	0.553	73.014	-2.735	-0.225	-0.698	no	no	no	0.436	no
28.	Tryptophan (Trp)	0.638	77.224	-2.735	-0.081	-0.495	no	no	no	0.640	no
29.	Valine (Val)	0.541	76.187	-2.736	0.572	0.354	no	no	no	0.205	no

VDss: Volume of supply at steady state; BBB: Blood-brain barrier; OCT2: Organic cation transporter 2.

interactions, predicting how bioactive compounds from ACE and ESMH may bind to key anti-inflammatory transduction signal targets (p38-MAPK), a key player in intracellular signaling pathways. In this study, the docking procedures were validated by employing native ligands Compound 10 for target protein p38-MAPK using AutoDock Vina with Lamarckian GA. The active site prediction for target proteins p38-MAPK gives the grid box coordinates (x y z) of 24.4628, 16.3186, and 10.6828, respectively. Molecular docking was carried out on native ligands (NL), 11 ACE metabolites, and 18 ESMH metabolites (Table 6). Based on the binding energy, all compounds can interact with the target receptor (PDB ID 3NEW).

Table 5. The toxicity prediction of *Ageratum conyzoides* metabolite and eggshell membrane hydrolysates using ProTox-3.0.

No.	Metabolite	Hepatotoxicity	Carcinogenicity	Mutagenicity	Cytotoxicity	Predicted LD_{50} (mg/kg)	Predicted Toxicity Class
	Native ligand Compound 10	No	No	No	No	135	3
	Diclofenac	Yes	No	No	No	53	3
	***Ageratum conyzoides* extract**						
1.	Quercetin-3-glucoside	No	No	No	No	5000	5
2.	Hyperoside	No	No	No	No	5000	5
3.	Monohydroxy-penta-methoxy-flavone	No	No	No	No	5000	5
4.	Astragaline / kaempferol 3-O-glucoside	No	No	No	No	5000	5
5.	Nobiletin	No	No	No	No	5000	5
6.	Kaempferol-7-O-rhamnopyranoside	No	Yes	No	No	5000	5
7.	Eupalestin	Yes	No	No	No	1190	4
8.	Luteolin	No	Yes	Yes	No	3919	5
9.	Quercetin-3-O-rutinoside	No	No	No	No	5000	5
10.	Luteolin-7-O-glucuronide	No	Yes	No	No	5000	5
11.	Apigenin	No	No	No	No	2500	5
	Eggshell membrane hydrolysate						
12.	Glycine (Gly)	No	No	No	No	3340	5
13.	Alanine (Ala)	No	No	No	No	2000	3
14.	Arginine (Arg)	No	No	No	No	7500	6
15.	Glutamic acid (Glu)	No	No	No	No	4500	5
16.	Aspartic acid (Asp)	No	No	No	No	923	4
17.	Phenylalanine (Phe)	No	No	No	No	2400	5
18.	Histidine (His)	No	No	No	No	15000	6
19.	Isoleucine (Ile)	No	No	No	No	10000	6
20.	Leucine (Leu)	No	No	No	No	10000	6
21.	Lysine (Lys)	No	No	Yes	No	366	4
22.	Methionine (Met)	No	No	No	No	4200	5
23.	Proline (Pro)	No	No	No	No	1000	4
24.	Serine (Ser)	No	No	No	No	2000	2
25.	Cysteine (Cys)	No	No	Yes	No	660	4
26.	Threonine (Thr)	No	No	No	No	12680	6
27.	Tyrosine (Tyr)	No	No	No	No	1460	4
28.	Tryptophan (Trp)	No	No	No	No	80	3
29.	Valine (Val)	No	No	No	No	12680	6

Table 6. The free energy of binding and inhibition constant of *Ageratum conyzoides* metabolite and eggshell membrane hydrolysates active site interaction on P38-MAPK (PDB ID 3NEW).

No.	Metabolite	Free energy of binding, ΔG (kcal/mol)	Inhibition constant, Ki (μM)
	Native Ligand Compound 10	-7.90	1.61
	Diclofenac	-8.07	1.22
	***Ageratum conyzoides* extract**		
1.	Quercetin-3-glucoside	-8.93	0.287
2.	Hyperoside	-9.06	0.228
3.	Monohydroxy-penta-methoxy-flavone	-9.53	0.104
4.	Astragaline / kaempferol 3-O-glucoside	-9.54	0.101
5.	Nobiletin	-8.92	0.291
6.	Kaempferol-7-O-rhamnopyranoside	-9.57	0.096
7.	Eupalestin	-8.48	0.607
8.	Luteolin	-9.43	0.123
9.	Quercetin-3-O-rutinoside	-6.84	9.66
10.	Luteolin-7-O-glucuronide	-9.03	0.242
11.	Apigenin	-8.72	0.406
	Eggshell membrane hydrolysate		
12.	Glycine (Gly)	-2.85	8200
13.	Alanine (Ala)	-3.38	3330
14	Arginine (Gly)	-4.04	1090
15.	Glutamic acid (Glu)	-2.52	14220
16.	Aspartic acid (Asp)	-2.15	26570
17.	Phenylalanine (Phe)	-5.26	139.37
18.	Histidine (His)	-3.82	1600
19.	Isoleucine (Ile)	-4.01	1160
20.	Leucine (Leu)	-4.11	970.78
21.	Lysine (Lys)	-4.02	1130
22.	Methionine (Met)	-3.77	1720
23.	Proline (Pro)	-4.21	826.80
24.	Serine (Ser)	-3.00	6350
25.	Cysteine (Cys)	-3.22	4360
26.	Threonine (Thr)	-3.46	2900
27.	Tyrosine (Tyr)	-5.16	165.84
28.	Tryptophan (Trp)	-6.10	33.74
29.	Valine (Val)	-3.64	2150

Notably, the ligand NL demonstrated a binding energy of -7.90 kcal/mol, resulting in an inhibition constant of 1.61 uM. This suggests a moderate binding affinity, indicating NL's potential as a ligand p38-MAPK. Other ligands, such as quercetin-3-glucoside, hyperoside, and monohydroxy-penta-methoxy-flavone demonstrated even stronger binding energies, ranging from -8.93 kcal/mol to -9.53 kcal/mol, with corresponding inhibition constants in the low nanomolar range (286.85 nM to 104.05 nM), indicating their high affinities for p38-MAPK. Kaempferol 3-O-glucoside and kaempferol-7-O-rhamnopyranoside exhibited particularly favorable binding energies of -9.54 kcal/mol and -9.57 kcal/mol, respectively, resulting in low inhibition constants of 100.85 nM and 95.84 nM. These findings suggest that these ligands may

have potent inhibitory effects on p38-MAPK. In contrast, ligands quercetin-3-O-rutinoside and apigenin displayed binding energies of -6.84 kcal/mol and -8.72 kcal/mol, translating to inhibition constants of 9.66 μM and 405.64 nM, respectively. While quercetin-3-O-rutinoside exhibited a weaker binding affinity, apigenin displayed a moderate affinity, highlighting the variability in ligand interactions within the ACE. Diclofenac and nobiletin exhibited binding energies of -8.07 kcal/mol and -8.92 kcal/mol, resulting in inhibition constants of 1.22 μM and 260.80 nM, respectively. These values suggest that diclofenac and nobiletin could serve as potential ligands with moderate to strong affinities for p38-MAPK. Amino acids and small molecules, including glycine, phenylalanine, threonine, and tryptophan, displayed binding energies ranging from -2.15 kcal/mol to -6.10 kcal/mol, with inhibition constants spanning from millimolar to micromolar ranges. These compounds demonstrated weaker interactions compared to the identified ligands from ACE, emphasizing the significance of natural product ligands.

The molecular docking investigation into ligand interactions with the target protein p38-MAPK (PDB ID 3NEW) unveiled intricate binding patterns involving hydrogen bonds (HB) and hydrophobic interactions (Fig. 2). The comprehensive analysis of these interactions provides valuable insights into the potential therapeutic relevance of the ligands and the stability of the complexes formed. NL, the native ligand, demonstrated a significant interaction profile with four hydrogen bonds involving Ser252, Ser251, and Lys249. Moreover, it engaged in an extensive 12 hydrophobic interactions with key residues Trp197, Ile250, Pro191, Ile259, Leu291, Leu195, Leu246, and Glu192. This detailed interaction network suggests NL's strong binding affinity, affirming its role as a crucial ligand for p38-MAPK. Quercetin-3-glucoside showcased an even more pronounced interaction profile, forming nine hydrogen bonds with Ser252, Lys249, Asp292, Ser293, Glu192, Leu291, Ile250, and Ser251. Additionally, it participated in 12 hydrophobic interactions with key residues such as Ala255, Trp197, Leu246, Ile250, Ser293, and Lys249. These findings emphasize the potential therapeutic significance of quercetin-3-glucoside in targeting p38-MAPK. Hyperoside, monohydroxy-penta-methoxy-flavone, and kaempferol 3-O-glucoside displayed varying degrees of interaction, forming six, seven, and seven hydrogen bonds, respectively. The hydrophobic interactions, ranging from 8 to 9, further contributed to their binding patterns. Key residues involved included Leu291, Ser233, Asp294, Ser252, Ser251, Glu192, and Ser293. These ligands exhibit considerable potential in forming stable complexes with p38-MAPK. Notably, ligands kaempferol-7-O-rhamnopyranoside, and eupalestin showed identical interaction patterns with five hydrogen bonds and six hydrophobic interactions. The involvement of key residues Ser293, Leu291, Ser252, and Asn196 in these interactions suggests a commonality in their binding mechanisms. Conversely, ligands luteolin and luteolin-7-O-glucuronide displayed a comparatively lower number of interactions. Luteolin formed four hydrogen bonds with Lys249, Ser252, and Leu291, accompanied by two hydrophobic interactions with Trp197 and Ile250. Luteolin-7-O-glucuronide, with six hydrogen bonds involving Lys249, Ser252, Leu291, Leu195, and Asn196, demonstrated three hydrophobic interactions with Trp197, Leu246, and Ile250. Diclofenac and nobiletin exhibited diverse interaction patterns. Diclofenac formed four hydrogen bonds and an extensive 13 hydrophobic interactions, highlighting its potential as a ligand with a different binding mode. This aligns with diclofenac's known inhibitory properties, hence validating the reliability of the docking approach. Nobiletin, with six hydrogen bonds and seven hydrophobic interactions, displayed a unique interaction profile, further emphasizing the diversity of ligand-protein binding.

The comprehensive analysis of ligand interactions with p38-MAPK (PDB ID 3NEW) provides valuable information for understanding the binding mechanisms and potential therapeutic applications of these ligands. The diverse interaction profiles of quercetin-3-glucoside and nobiletin from ACE suggest promising candidates for further investigation.

DISCUSSION

Inflammation is one of the body's defense responses, aiming to eliminate the cause of tissue or cell injury, cleanse the tissue of residual damage, and build new tissue. The triggers of inflammation can be either infectious or non-infectious. Infectious factors leading to inflammation encompass bacteria, viruses, and other microorganisms, while non-infectious factors can result from physical sources, chemical compounds, or biological elements. Physical inducers include burns, radiation, trauma, foreign bodies, and injuries. Chemical compounds capable of inducing inflammation range from glucose, fatty acids, toxins, and alcohol to irritants. Additionally, biologically damaged cells have the potential to initiate inflammatory responses (Chen et al., 2018). In this study, the induction of cotton pellets was used by a mechanism such as physical induction of foreign bodies and physical induction. At present, the use of foreign materials for health has increased and will continue, one of which is with the expansion of biomaterial applications and rapid aging population expansion. One of the main factors that limit its use is the response of

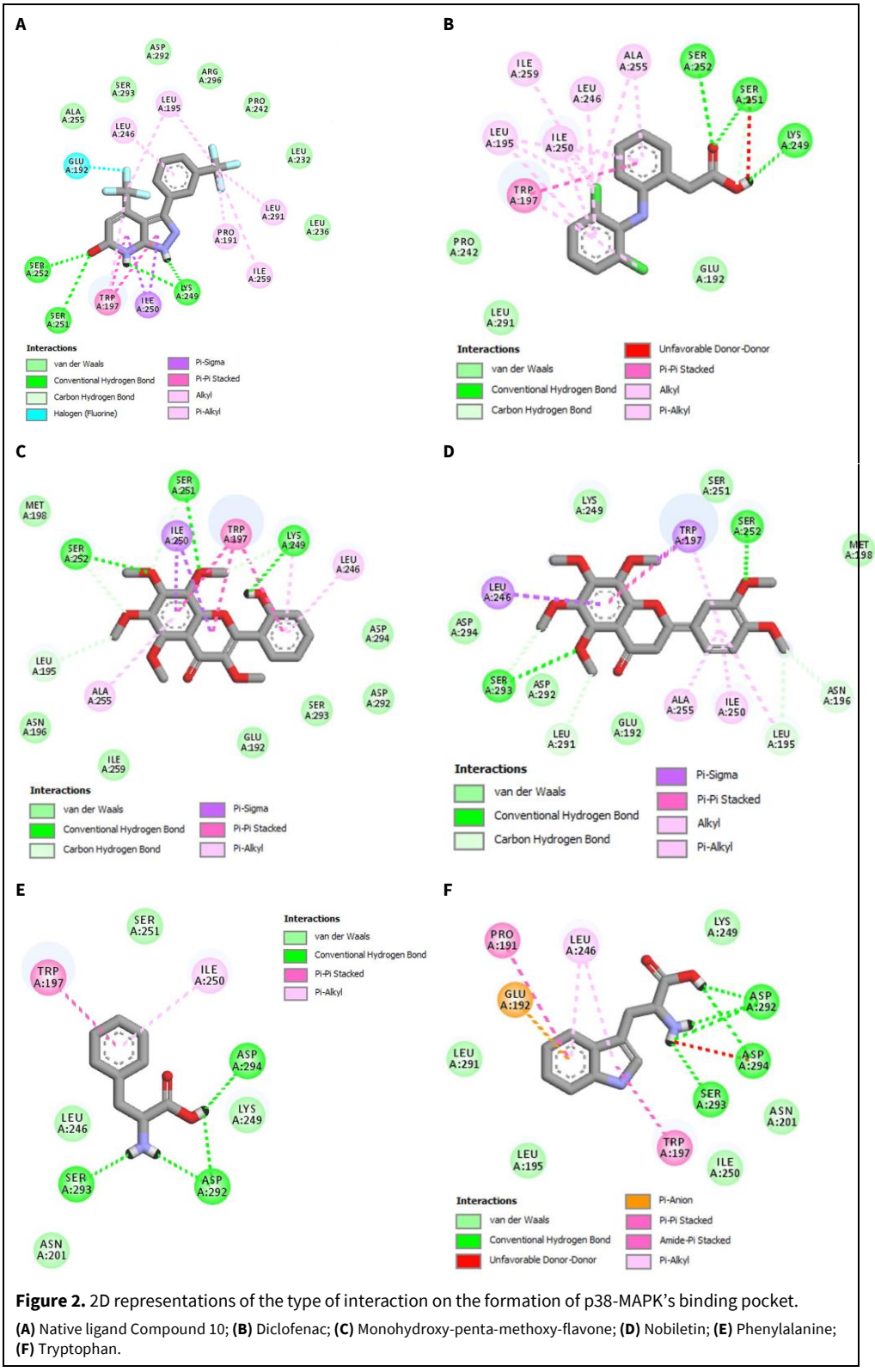

Figure 2. 2D representations of the type of interaction on the formation of p38-MAPK's binding pocket.

(A) Native ligand Compound 10; **(B)** Diclofenac; **(C)** Monohydroxy-penta-methoxy-flavone; **(D)** Nobiletin; **(E)** Phenylalanine; **(F)** Tryptophan.

foreign objects, immunological reactions characterized by chronic inflammation, the formation of giant foreign objects, and the formation of fibrotic capsules (Major et al., 2015; Mariani et al., 2019). Consequently, there is a need to broaden research on chronic anti-inflammatory measures in the context of foreign object induction.

In the initial stages of inflammation, leucocytes recognize pathogen-associated molecular patterns (PAMPs), triggering alterations in mitochondrial dynamics and function. This mitochondrial response

prompts leukocytes to release pro-inflammatory cytokines (Missiroli et al., 2020). Leukocytes will also release lysosomal enzymes such as proteases (Ansar and Ghosh, 2016). In this study, the membrane stabilization effect was tested using RBC because the RBC membrane is identical to the leucocyte membrane. Preventing RBC hemolysis is identified as having the ability to inhibit leukocyte membrane lysis and inhibit the inflammatory process (Gunathilake et al., 2018). The anti-inflammatory effects of ACE and ESMH were reinforced by their capacity to stabilize membranes. The ability of ACE to stabilize membranes is assumed to be caused by its ability to increase the activity of NADH dehydrogenase and cytochrome c oxidase in the inner mitochondrial membrane, the two of which are involved in the synthesis of ATP energy and thus contribute to membrane stabilization (Elangovan et al., 2020). Nobiletin found in *Citrus nobilis* peel extract has a similar effect as a membrane stabilizer (Malik et al., 2021). Quercetin and kaempferol in *Moringa oleifera* also had ability to stabilize membrane (Saleem et al., 2020). While the precise effects of other components in ACE on membrane stabilization are undetermined, it is hypothesized that they contribute to this process.

The membrane stabilization test was carried out using hypotonic solution induction. Hypotonic induction will cause cells to experience oxidative stress, resulting in an imbalance in the number of free radicals, causing membrane fluidity, increasing membrane leakage, and damaging membrane proteins, thereby inactivating receptors, enzymes, and ion channels (Biswas, 2016). Hydrophobic amino acids (Leu, Val, Ala, Pro, Phe, His, Trp, Gly, Lys, and Ile) and aromatic amino acids (Phe, Trp, and Tyr) are present in ESM/ESMH and have been shown in previous studies to act as antioxidants (Zhu et al., 2022a). The mechanism of ESM as an antioxidant is thought to be related to the activation of the Elch-like ECH-associated protein 1 (Keap1) pathway, which binds to the nuclear factor erythroid 2-related factor 2 (Nrf2) (Zhu et al., 2022b). The antioxidant effects of ACE and ESM/ESMH are thought to support membrane stabilizing effects, which further influence the inflammation process.

The next phase in the inflammation process is that leucocytes will experience margination, rolling, adhesion to endothelial cells, passing through endothelial gaps (diapedesis), and movement of leukocytes to the location of the area that triggers the inflammatory response. Cells will also respond by releasing pro-inflammatory mediators (Ansar and Ghosh, 2016). Margination occurs when the flowing leukocytes stop because they have a suitable bond with the endothelium in the capillaries. During the margination, leukocyte cells will bind to vascular adhesion molecule-1 (VCAM-1) and ICAM-1 (immunoglobulin ligands). The leukocyte cells that bind to endothelial cells will change shape to become slightly flatter (pavementing of leucocytes), which makes it easier for them to pass through the gaps of the endothelial cells and exit into the tissue (Ansar and Ghosh, 2016). ESM powder and its carbohydrate fraction can reduce the transcription factor NF-κB and down-regulate the expression of the immune regulating receptors toll-like receptor 4 and ICAM-1, as well as the cell surface glycoprotein CD44 (Vuong et al., 2017).

Both ACE and ESMH demonstrated the ability to inhibit albumin/protein denaturation., a phenomenon also observed with NSAID diclofenac-Na in this study. Protein denaturation can occur due to physical injuries heat, acid or alkaline solutions, electrolytes, alcohol, and other compounds that change the solubility of albumin and globulin. During inflammation, the accumulation of leukocytes in the affected area may occur due to increased blood vessel permeability resulting from protein denaturation when essential compounds needed to address the source of inflammation are perceived to be lacking (OPIE, 1962; Osman et al., 2016). Quercetin and kaempferol in *Moringa oleifera* have the effect of inhibiting protein denaturation, preventing inflammation and anemia in test animals (Saleem et al., 2020). *Citrus nobilis* peel extract contains nobiletin, sinensetin, and tangeritin and shows the effect of inhibiting protein denaturation (Malik et al., 2021). It is suspected that quercetin, kaempferol, and nobiletin compounds contained in ACE contribute to inhibiting protein denaturation. The essential amino acids Arg, Tyr, His, and Phe present in fermented soybeans can decrease protein denaturation activity (Ketnawa and Ogawa, 2019), therefore it is assumed that ESMH possesses the same amino acids that can inhibit protein denaturation.

Neutrophils contribute significantly to the inflammatory process. They play a pivotal role in recruiting monocytes and activating macrophages for phagocytosis, the generation of pro-inflammatory reactive oxygen species (ROS) and neutrophil extracellular traps (NETs), as well as proteolytic activities (Castanheira and Kubes, 2019). Proteolytic activity is mediated by the neutrophil serine protease enzyme, namely cathepsin G (CG), neutrophil elastase (NE), and proteinase 3 (PR3). Neutrophils secreting excessive protease will disrupt the delicate balance with antiproteases in the environment. CG plays a role in the activation and production of IL-8, TNFα, and IL-1β cytokines. PR3 modulates immune responses by activating pro-inflammatory cytokines and controlling cellular activities. Moreover, PR3 actively promotes the release of cytokines such as TNF-α, IL-1,

TGF, and IL-8. The absence of NE was related to lower levels of pro-inflammatory cytokines such as TNF-α, macrophage inflammatory protein-2 (MIP-2), and IL-6. Since antiproteases play a crucial role in the regulation of proteases, an absence of these may result in prolonged, uncontrollable protease activity, which, in consequence, may trigger tissue damage and inflammation (Oriano et al., 2021; Stockley, 1999). In this study, ACE and ESMH had antiprotease activity. The flavonoid content in ACE is thought to have this effect. Quercetin can improve the protease-antiprotease balance by restraining the severity of inflammation in animal models of chronic obstructive pulmonary disease induced by elastase/lipopolysaccharide (LPS) (Ganesan et al., 2010). Autophagy, one of the proteolytic mechanisms occurring within the lysosomal system, is responsible for the degradation of endogenous proteins. Plasma amino acids physiologically regulate the autophagy system via a signal transduction mechanism. Several amino acids, including Leu, Gln, Tyr, Phe, Pro, Met, Trp, and His in the liver and Leu in the skeletal muscle, have a direct regulatory potential in autophagic proteolysis. The recognition of these amino acids at the plasma membrane indicates an amino acid receptor or sensor may be present, which will be vital to their recognition and resulting intracellular signaling (Kadowaki and Kanazawa, 2003). The amino acid content in ESMH is observed to influence the autophagy signaling pathway and proteolysis process, but this needs to be confirmed with further research.

Chronic inflammation is characterized by a prolonged influx of neutrophils and NETs release (Soehnlein et al., 2017). Neutrophils can be used as anti-inflammatory targets by reducing the release of NETs (Klopf et al., 2021). In chronic inflammation, NE and PR3 will inactivate the anti-inflammatory mediator progranulin (Kessenbrock et al., 2011). Although the exact number of neutrophils in this study was not determined, it is apparent that the administration of ACE, ESMH, and their combination could have lowered the number of granulocytes as compared with controls.

Platelets are another blood cell component that plays a role in the inflammatory process. Platelets can modulate the function of endothelial cells and leukocytes (neutrophils) and regulate the function of macrophages and lymphocyte cells (Jenne et al., 2013). Platelets influence vascular permeability and recruitment of neutrophils and/or macrophages. Activated platelets will express P-selectin on their cell surface, which can interact with the selectin receptor PSGL-1 expressed on leukocytes. Platelets influence leukocyte emigration by capturing leukocytes at specific extravasation sites. Platelets will also interact with monocytes, where the resulting complex will induce a pro-inflammatory phenotype in monocytes (Gros et al., 2015). Platelets also influence the inflammatory response of leukocytes by stimulating the secretion of pro-inflammatory cytokines (Klinger, 1997). Patients with chronic inflammatory diseases change thrombopoietin levels. Psoriasis sufferers experience an increase in mean platelet volume, platelet distribution width, soluble P-selectin levels, and platelet aggregation. In chronic inflammation, inhibiting thrombopoietin function can protect and reduce organ damage (Margraf and Zarbock, 2019). In this study, diclofenac-Na demonstrated the ability to reduce platelet counts compared to controls. The combination use of ACE and ESMH is additive in reducing platelet counts compared to individual use. The methanol extract of *A. conyzoides* showed a reduction in bleeding time, clotting time, and plasma fibrinogen concentration, suggesting a decrease in platelet activity (Bamidele et al., 2010).

Another cell that plays a role in inflammation is macrophages. Activated monocytes will become macrophages. Based on the stimulus they receive, macrophages are divided into two, namely M1 (pro-inflammatory) and M2 (anti-inflammatory). In acute inflammation, M1 will be stimulated by lipopolysaccharides, PAMPs/DAMPs, IFN-β, and IFN-γ so that it secretes pro-inflammatory cytokines (Hamidzadeh et al., 2017). Then, there will be a transition from changing M1 to M2. If this transition is missed, excessive M1 can be harmful and cause lesions and chronic inflammation (Lee and Choi, 2018). ACE may prevent macrophage cells from producing prostaglandin E and nitric oxide (Seemakhan and Srisook, 2014). Nobiletin (3,5,6,7,3′,4′-hexamethoxyflavone) inhibits macrophage cells from producing the cytokines interleukin (IL)-6, IL-1β, TNF-α, and NF-κB. Nobiletin can inhibit the inflammatory response in the ERK pathway by inhibiting the phosphorylation of the ERK protein (Son et al., 2020). In this study, mid-sized cells (monocytes and basophilic granulocytes) (Roleff et al., 2007) were measured. Although M1 and M2 cannot be differentiated, based on the results, it is suspected that ACE inhibits M1 proliferation occurs through the ERK pathway.

MAPK is capable of activating a wide variety of biological effects in response to prior stimuli. In the chronic inflammatory process induced by cotton pellets, inflammation is caused by the stress-activated protein kinase (SAPK) and the p-38 kinase pathway, especially in macrophages. The p38-MAPK signaling system can be activated by UV light, higher extracellular osmolality, pro-inflammatory cytokines, or harmful microbial products. The p38-MAPK family includes p38α, p38β, p38γ, and p38δ. p38α and

p38beta are found in practically all cells; p38γ is detected in muscle, and p38δ is expressed in the lungs, pancreas, kidneys, testes, and small intestine. Activation of p38-MAPK leads to the generation of pro-inflammatory cytokines (TNF-α, IL-1, IL-6, TGFβ) and oxidative stress (Kaminska, 2005; Yang et al., 2014). ACE and ESMH testing of p38-MAPK activity was conducted in this study using *in silico* molecular docking.

In molecular docking, the interaction of compounds with p38-MAPK is assessed using binding energy and Ki. Binding energy is the energy released when a ligand binds to a receptor protein, while Ki represents the ligand-receptor complex dissociation constant, indicating the concentration needed to cover 50% of the receptor binding site. The binding selectivity and affinity of ligands to receptor proteins are predicted using binding energy and Ki. To assess the strength of the interaction and compare the binding affinities of different ligands, molecular docking studies frequently report the binding energy and Ki values of the docked ligand-receptor complex (Aligita et al., 2023; Du et al., 2016). Molecular docking results indicate that the ACE substances possess low to high-binding energies for p38-MAPK. High-binding energy compounds include quercetin-3-glucoside, hyperoside, and monohydroxy-penta-methoxy-flavone; medium-binding energy compounds include kaempferol 3-O-glucoside and kaempferol-7-O-rhamnopyranoside; and low binding energy compounds include quercetin-3-O-rutinoside and apigenin. Nobiletin could serve as a potential ligand with moderate to strong affinity for p38-MAPK. Compared to the identified ligands from ACE, amino acids and small molecules, such as glycine, phenylalanine, threonine, and tryptophan, in ESMH have weaker interactions; however, the combination of the two as natural product ligands p38-MAPK needs to be considered. Fig. 3 illustrates the hypothesis that ACE and ESMH may have an additive effect on chronic inflammation.

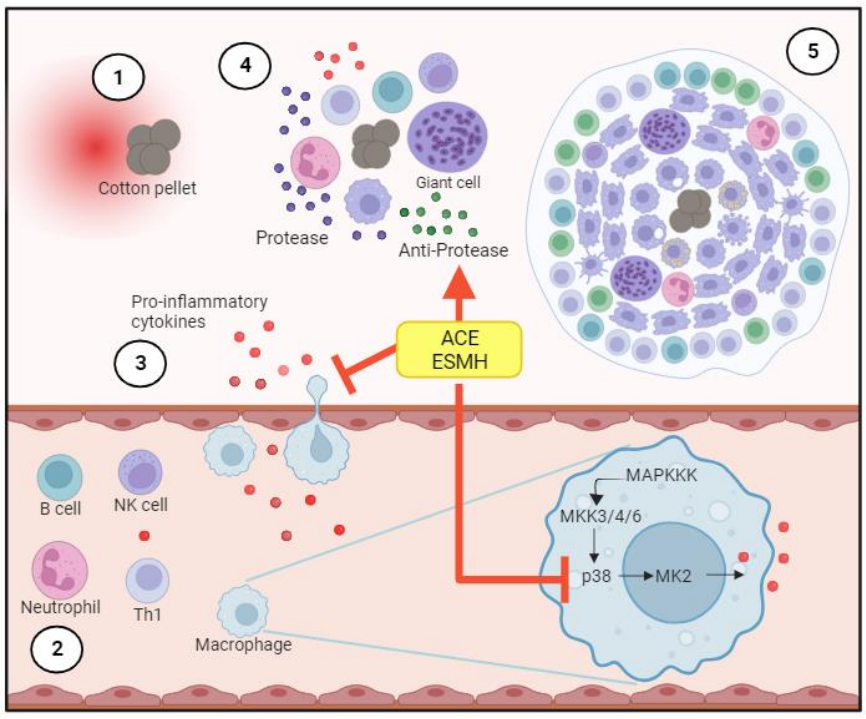

Figure 3. Hypothesis on the mechanism of action of *Ageratum conyzoides* extract and the eggshell membrane hydrolysates in preventing chronic inflammation.

(1) Inflammation is caused by cotton pellets; **(2)** Cells in blood vessels (neutrophil cells, macrophage cells, T lymphocyte cells, B lymphocyte cells, and NK cells) respond and release pro-inflammatory cytokines as the consequence of cell signal transduction, one of which is on the p38-MAPK pathway, which induces pro-inflammatory cytokine secretion; **(3)** Vasodilation occurs to enable cells to do diapedesis and move to the tissue surrounding an injury; **(4)** There is an imbalance of protease-antiprotease and in chronic inflammation, cells that gather in the inflammatory area will form giant cells; **(5)** Granulomas will be formed by merging of giant cells. *A. conyzoides* extract and eggshell membrane hydrolysates will work additively to stabilize the membrane, regulate the equilibrium of protease-antiprotease, and inhibit the p38-MAPK signal transduction. Created with BioRender.com.

The evaluation of pharmacokinetic and toxicity profiles, which are currently easy to predict through computational methods, is a crucial aspect of drug development. One usual criterion for drug-likeness analysis is Lipinski's rule of five. The original Lipinski's rule of five defines four basic physicochemical parameter ranges and is valid for orally active compounds (Lipinski, 2004). All the amino acids in ESMH meet the Lipinski rule's drug-likeness standards. This means that all the amino acids can be taken orally and be absorbed well. However, some compounds in ACE do not follow Lipinski's five rules. A compound that does not fit Lipinski's rule of five can be delivered by non-oral routes such as pulmonary, intra nasal, or dermal (Lipinski, 2004). This study applied an oral administration of the ACE and ESMH mixture. However, considering the favorable skin permeability of the compounds in ACE and the predicted absorption profile of all amino acids in ESMH, further investigation is required regarding the topical or transdermal application of the mixture.

Based on a computational study, most amino acids in ESMH and all ACE components are known not to cross the blood-brain barrier. In theory, this will affect its ability to overcome systemic inflammatory diseases, where, during systemic inflammation, there will be changes in the permeability of the BBB. Vascular blood-brain barrier permeability to solutes, lymphocyte trafficking, and innate immune cell infiltration all increase in association with the severity and duration of systemic inflammation (Galea, 2021). In this study, a mixture of ESMH and ACE was able to treat systemic inflammatory conditions, but it is not yet known whether it can cross the BBB. Therefore, it is necessary to study more deeply the ability of the compounds in ESMH and ACE to cross the BBB in inflammatory conditions, either in silico, *in vitro* or *in vivo* using animal models. The metabolic process in the liver has an impact on the efficacy of a drug. In this study, several compounds in ACE were found to inhibit the CYP450 enzyme. The inhibitory effect on the action of the CYP450 enzyme can cause synergistic effects (especially the use of herbal mixtures), treatment failure, or increased serious side effects. Apart from that, it also has the potential to cause drug interactions (Adianingsih et al., 2022; Zuo et al., 2022).

The drug can be used for a short or long period of time and is not expected to cause toxicity. The adverse outcomes that need to be considered are cytotoxic, hepatotoxic, and cancerous. The liver plays a significant role in minimizing the harmful effects of drugs. Hepatotoxic compounds have the ability to harm the liver, resulting in organ failure or potentially causing death. Therefore, it is crucial to carefully evaluate the potential for liver damage during the process of developing and discovering new drugs (Adianingsih et al., 2022).

CONCLUSION

The administration of *A. conyzoides* extract, eggshell membrane hydrolysates, and their mixture was proven to be additive in inhibiting the formation of exudates and granulomas, as well as reducing the severity of chronic inflammation in test animals produced from cotton pellets with several working actions. Individual or combined administration will reduce the number of leukocytes, lymphocytes, mid-sized cells, and granulocytes. *In vitro* testing shows that this anti-inflammatory effect can be due to the ability to increase membrane stability, reduce protein denaturation, and modify the protease-antiprotease balance from the initial phase of inflammation to chronic inflammation. However, since the precise relationship between *A. conyzoides* extract and eggshell membrane hydrolysates at each stage is still unknown, further research with specific techniques is necessary. *In silico* analysis indicates that the combination of ACE and ESMH impacts the p38-MAPK signaling pathway, which is associated with inflammation. Subsequent studies utilizing cell cultures are expected to validate these findings.

CONFLICT OF INTEREST

The authors declare no conflicts of interest.

ACKNOWLEDGMENTS

The authors acknowledge the support provided by the Indonesian Endowment Fund for Education (LPDP, *Lembaga Pengelola Dana Pendidikan*) No. KET-159/LPDP.4/2021 in conducting this study.

REFERENCES

Adianingsih OR, Khasanah U, Anandhy, Yurina V (2022) *In silico* ADME-T and molecular docking study of phytoconstituents from *Tithonia diversifolia* (Hemsl.) A. Gray on various targets of diabetic nephropathy. J Pharm Pharmacogn Res 10(4): 571–594. https://doi.org/10.56499/jppres22.1345.10.4.571

Aligita W, Singgih M, Sutrisno E, Adnyana IK (2023) Hepatoprotective study of Indonesian water kefir against CCl4-induced liver injury in rats. J Pharm Pharmacogn Res 11(6): 1002–1016. https://doi.org/10.56499/jppres23.1732_11.6.1002

Ansar W, Ghosh S (2016) Inflammation and inflammatory diseases, markers, and mediators: Role of CRP in some inflammatory diseases. In: Biology of C Reactive Protein in Health and Disease. New Delhi: Springer, pp. 67–107. https://doi.org/10.1007/978-81-322-2680-2_4

Asnawi A, Nedja M, Febrina E, Purwaniati P (2023) Prediction of a stable complex of compounds in the ethanol extract of celery leaves (*Apium graveolens* L.) function as a VKORC1 antagonist. Trop J Nat Prod Res 7(2): 2362-2370. https://doi.org/10.26538/tjnpr/v7i2.10

AL Azzam K (2023) SwissADME and pkCSM webservers predictors: An integrated online platform for accurate and comprehensive predictions for *in silico* ADME/T properties of artemisinin and its derivatives. Compl Use Min Resour 325(2): 14–21. https://doi.org/10.31643/2023/6445.13

Bamidele O, Akinnuga AM, Anyakudo MMC, Ojo OA, Ojo GB, Olorunfemi OJ, Johnson OP (2010) Haemostatic effect of methanolic leaf extract of *Ageratum conyzoides* in albino rats. J Med Plant Res 4(20): 2075–2079.

Banerjee P, Eckert AO, Schrey AK, Preissner R (2018) ProTox-II: a webserver for the prediction of toxicity of chemicals. Nucleic Acids Res 46(W1): W257-W263. https://doi.org/10.1093/nar/gky318

Bayraktar O, Galanakis CM, Aldawoud TMS, Ibrahim SA, Köse MD, Uslu ME (2021) Utilization of eggshell membrane and olive leaf extract for the preparation of functional materials. Foods 10(4): 806. https://doi.org/10.3390/foods10040806

Biswas SK (2016) Does the interdependence between oxidative stress and inflammation explain the antioxidant paradox? Oxid Med Cell Longev 2016: 5698931. https://doi.org/10.1155/2016/5698931

Caesar LK, Cech NB (2019) Synergy and antagonism in natural product extracts: when 1 + 1 does not equal 2. Nat Prod Rep 36(6): 869-888. https://doi.org/10.1039/c9np00011a

Cánovas F, Abellán-Ruíz MS, García-Muñoz AM, Luque-Rubia AJ, Victoria-Montesinos D, Pérez-Piñero S, Sánchez-Macarro M, López-Román FJ (2022) Randomised clinical trial to analyse the efficacy of eggshell membrane to improve joint functionality in knee osteoarthritis. Nutrients 14(11): 2340. https://doi.org/10.3390/nu14112340

Castanheira FVS, Kubes P (2019) Neutrophils and NETs in modulating acute and chronic inflammation. Blood 133(20): 2178–2185. https://doi.org/10.1182/blood-2018-11-844530

Chen L, Deng H, Cui H, Fang J, Zuo Z, Deng J, Li Y, Wang X, Zhao L (2018) Inflammatory responses and inflammation-associated diseases in organs. Oncotarget 9(6): 7204-7218. https://doi.org/10.18632/oncotarget.23208

Choi HJ, Kim YM, Suh JY, Han JY (2021) Beneficial effect on rapid skin wound healing through carboxylic acid-treated chicken eggshell membrane. Mater Sci Eng C Mater Biol Appl 128: 112350. https://doi.org/10.1016/j.msec.2021.112350

Clarke TC, Black LI, Stussman BJ, Barnes PM, Nahin RL (2015) Trends in the use of complementary health approaches among adults: United States, 2002–2012. Natl Health Stat Report (79): 1-16. https://www.ncbi.nlm.nih.gov/pmc/articles/PMC4573565/

Daina A, Michielin O, Zoete V (2017) SwissADME: A free web tool to evaluate pharmacokinetics, drug-likeness and medicinal chemistry friendliness of small molecules. Sci Rep 7(1): 42717. https://doi.org/10.1038/srep42717

Du X, Li Y, Xia YL, Ai SM, Liang J, Sang P, Ji XL, Liu SQ (2016) Insights into protein-ligand interactions: mechanisms, models, and methods. Int J Mol Sci 17(2): 144. https://doi.org/10.3390/ijms17020144

Elangovan B, Ajayakumar AS, Anandraj RP (2020) Cardioprotective role of *Ageratum conyzoides* L. on cardiac mitochondrial enzymes during isoproterenol-induced myocardial infarction in rats. Int J Pharmacognosy Pharm Sci 2(2): 9–13. https://doi.org/10.33545/27067009.2020.v2.i2a.64

Fathihah B, Mahmood AA, Sidik K, Salmah I (2005) The Antiulcer and cytoprotective effect of *Ageratum conyzoides*' honey combination in rats. J Health Trans Med 8(1): 28–32. https://doi.org/10.22452/jummec.vol8no1.6

Fuhrmann J, Rurainski A, Lenhof HP, Neumann D (2010) A new Lamarckian genetic algorithm for flexible ligand-receptor docking. J Comput Chem 31(9): 1911-1918. https://doi.org/10.1002/jcc.21478

Galea I (2021) The blood-brain barrier in systemic infection and inflammation. Cell Mol Immunol 18(11): 2489-2501. https://doi.org/10.1038/s41423-021-00757-x

Ganesan N, Ronsmans S, Vanoirbeek J, Hoet PHM (2022) Assessment of experimental techniques that facilitate human granuloma formation in an *in vitro* system: A systematic review. Cells 11(5): 864. https://doi.org/10.3390/cells11050864

Ganesan S, Faris AN, Comstock AT, Chattoraj SS, Chattoraj A, Burgess JR, Curtis JL, Martinez FJ, Zick S, Hershenson MB, Sajjan US (2010) Quercetin prevents progression of disease in elastase/LPS-exposed mice by negatively regulating MMP expression. Respir Res 11(1): 131. https://doi.org/10.1186/1465-9921-11-131

Gros A, Ollivier V, Ho-Tin-Noé B (2015) Platelets in inflammation: Regulation of leukocyte activities and vascular repair. Front Immunol 5: 678. https://doi.org/10.3389/fimmu.2014.00678

Gunathilake KDPP, Ranaweera KKDS, Rupasinghe HPV (2018) *In vitro* anti-inflammatory properties of selected green leafy vegetables. Biomedicines 6(4): 107. https://doi.org/10.3390/biomedicines6040107

Hamidzadeh K, Christensen SM, Dalby E, Chandrasekaran P, Mosser DM (2017) Macrophages and the recovery from acute and chronic inflammation. Annu Rev Physiol 79: 567-592. https://doi.org/10.1146/annurev-physiol-022516-034348

Jain S, Anal AK (2017) Production and characterization of functional properties of protein hydrolysates from egg shell membranes by lactic acid bacteria fermentation. J Food Sci Technol 54(5): 1062-1072. https://doi.org/10.1007/s13197-017-2530-y

Jenne CN, Urrutia R, Kubes P (2013) Platelets: bridging hemostasis, inflammation, and immunity. Int J Lab Hematol 35(3): 254-261. https://doi.org/10.1111/ijlh.12084

Jia H, Hanate M, Aw W, Itoh H, Saito K, Kobayashi S, Hachimura S, Fukuda S, Tomita M, Hasebe Y, Kato H (2017) Eggshell membrane powder ameliorates intestinal inflammation by facilitating the restitution of epithelial injury and alleviating microbial dysbiosis. Sci Rep 7: 43993. https://doi.org/10.1038/srep43993

Kadowaki M, Kanazawa T (2003) Amino acids as regulators of proteolysis. J Nutr 133(6 Suppl 1): 2052S-2056S. https://doi.org/10.1093/jn/133.6.2052S

Kamala Lakshmi B, Valarmathi S (2020) *In vitro* anti-inflammatory activity of aqueous extract of Albizia lebbeck leaf (L). J Phytopharmacol 9(5): 356-360. https://doi.org/10.31254/phyto.2020.9511

Kaminska B (2005) MAPK signalling pathways as molecular targets for anti-inflammatory therapy--from molecular mechanisms to therapeutic benefits. Biochim Biophys Acta 1754(1-2): 253-262. https://doi.org/10.1016/j.bbapap.2005.08.017

Kemppainen LM, Kemppainen TT, Reippainen JA, Salmenniemi ST, Vuolanto PH (2018) Use of complementary and alternative medicine in Europe: Health-related and sociodemographic determinants. Scand J Public Health 46(4): 448-455. http://doi.org/10.1177/1403494817733869

Kessenbrock K, Dau T, Jenne DE (2011) Tailor-made inflammation: How neutrophil serine proteases modulate the inflammatory response. J Mol Med (Berl) 89(1): 23-28. https://doi.org/10.1007/s00109-010-0677-3

Ketnawa S, Ogawa Y (2019) Evaluation of protein digestibility of fermented soybeans and changes in biochemical characteristics of digested fractions. J Funct Foods 52: 640–647. https://doi.org/10.1016/j.jff.2018.11.046

Kiers JL, Bult JHF (2021) Mildly processed natural eggshell membrane alleviates joint pain associated with osteoarthritis of the knee: A randomized double-blind placebo-controlled study. J Med Food 24(3): 292-298. https://doi.org/10.1089/jmf.2020.0034

Kim EK, Choi EJ (2015) Compromised MAPK signaling in human diseases: An update. Arch Toxicol 89(6): 867-882. https://doi.org/10.1007/s00204-015-1472-2

Klinger MH (1997) Platelets and inflammation. Anat Embryol (Berl) 196(1): 1-11. https://doi.org/10.1007/s004290050075

Klopf J, Brostjan C, Eilenberg W, Neumayer C (2021) Neutrophil extracellular traps and their implications in cardiovascular and inflammatory disease. Int J Mol Sci 22(2): 559. https://doi.org/10.3390/ijms22020559

Kotta JC, Lestari ABS, Candrasari DS, Hariono M (2020) Medicinal effect, *in silico* bioactivity prediction, and pharmaceutical formulation of *Ageratum conyzoides* L.: A review. Scientifica 2020: 6420909. https://doi.org/10.1155/2020/6420909

Laveti D, Kumar M, Hemalatha R, Sistla R, Naidu VG, Talla V, Verma V, Kaur N, Nagpal R (2013) Anti-inflammatory treatments for chronic diseases: A review. Inflamm Allergy Drug Targets 12(5): 349-361. https://doi.org/10.2174/18715281113129990053

Lee CH, Choi EY (2018) Macrophages and Inflammation. J Rheum Dis 25: 11-18. https://doi.org/10.4078/jrd.2018.25.1.11

Lee D, Bamdad F, Khey K, Sunwoo HH (2017) Antioxidant and anti-inflammatory properties of chicken egg vitelline membrane hydrolysates. Poult Sci 96(9): 3510-3516. https://doi.org/10.3382/ps/pex125

Li X, Cai Z, Ahn DU, Huang X (2019) Development of an antibacterial nanobiomaterial for wound-care based on the absorption of AgNPs on the eggshell membrane. Colloids Surf B Biointerfaces 183: 110449. https://doi.org/10.1016/j.colsurfb.2019.110449

Lindvall JM, Blomberg KE, Smith CI (2003) *In silico* tools for signal transduction research. Brief Bioinform 4(4): 315-324. https://doi.org/10.1093/bib/4.4.315

Lipinski CA (2004) Lead- and drug-like compounds: the rule-of-five revolution. Drug Discov Today Technol 1(4): 337–341. https://doi.org/10.1016/j.ddtec.2004.11.007

Major MR, Wong VW, Nelson ER, Longaker MT, Gurtner GC (2015) The foreign body response: at the interface of surgery and bioengineering. Plast Reconstr Surg 135(5): 1489-1498. https://doi.org/10.1097/PRS.0000000000001193

Malik A, Najda A, Bains A, Nurzyńska-Wierdak R, Chawla P (2021) Characterization of *Citrus nobilis* peel methanolic extract for antioxidant, antimicrobial, and anti-inflammatory activity. Molecules 26(14): 4310. https://doi.org/10.3390/molecules26144310

Margraf A, Zarbock A (2019) Platelets in inflammation and resolution. J Immunol 203(9): 2357-2367. https://doi.org/10.4049/jimmunol.1900899

Mariani E, Lisignoli G, Borzì RM, Pulsatelli L (2019) Biomaterials: Foreign Bodies or Tuners for the Immune Response? Int J Mol Sci 20(3): 636. https://doi.org/10.3390/ijms20030636

Missiroli S, Genovese I, Perrone M, Vezzani B, Vitto VAM, Giorgi C (2020) The role of mitochondria in inflammation: From cancer to neurodegenerative disorders. J Clin Med 9(3): 740. https://doi.org/10.3390/jcm9030740

Moreno-Fernández S, Garcés-Rimón M, Miguel M (2020) Egg-derived peptides and hydrolysates: A new bioactive treasure for cardiometabolic diseases. Trends Food Sci Technol 104: 208–218. https://doi.org/10.1016/j.tifs.2020.08.002

Moura ACA, Silva ELF, Fraga MCA, Wanderley AG, Afiatpour P, Maia MBS (2005) Antiinflammatory and chronic toxicity study of the leaves of *Ageratum conyzoides* L. in rats. Phytomedicine 12(1–2): 138–142. https://doi.org/10.1016/j.phymed.2003.12.003

OPIE EL (1962) On the relation of necrosis and inflammation to denaturation of proteins. J Exp Med 115(3): 597-608. https://doi.org/10.1084/jem.115.3.597

Oriano M, Amati F, Gramegna A, De Soyza A, Mantero M, Sibila O, Chotirmall SH, Voza A, Marchisio P, Blasi F, Aliberti S (2021) Protease-antiprotease imbalance in bronchiectasis. Int J Mol Sci 22(11): 5996. https://doi.org/10.3390/ijms22115996

Osman NI, Sidik NJ, Awal A, Adam NA, Rezali NI (2016) *In vitro* xanthine oxidase and albumin denaturation inhibition assay of *Barringtonia racemosa* L. and total phenolic content analysis for potential anti-inflammatory use in gouty arthritis. J Intercult Ethnopharmacol 5(4): 343-349. https://doi.org/10.5455/jice.20160731025522

Paul S, Datta BK, Ratnaparkhe MB, Dholakia BB (2022) Turning waste into beneficial resource: Implication of *Ageratum conyzoides* L. in sustainable agriculture, environment and biopharma sectors. Mol Biotechnol 64(3): 221-244. https://doi.org/10.1007/s12033-021-00409-5

Pires DE, Blundell TL, Ascher DB (2015) pkCSM: Predicting small-molecule pharmacokinetic and toxicity properties using graph-based signatures. J Med Chem 58(9): 4066-4072. https://doi.org/10.1021/acs.jmedchem.5b00104

Pober JS, Sessa WC (2015) Inflammation and the blood microvascular system. Cold Spring Harb Perspect Biol 7(1): a016345. https://doi.org/10.1101/cshperspect.a016345

Rafiyan M, Sadeghmousavi S, Akbarzadeh M, Rezaei N (2023) Experimental animal models of chronic inflammation. Curr Res Immunol 4: 100063. https://doi.org/10.1016/j.crimmu.2023.100063

Roleff S, Arndt G, Bottema B, Junker L, Grabner A, Kohn B (2007) Clinical evaluation of the CA530-VET hematology analyzer for use in veterinary practice. Vet Clin Pathol 36(2): 155-166. https://doi.org/10.1111/j.1939-165X.2007.tb00202.x

Ruff KJ, Morrison D, Duncan SA, Back M, Aydogan C, Theodosakis J (2018) Beneficial effects of natural eggshell membrane versus placebo in exercise-induced joint pain, stiffness, and cartilage turnover in healthy, postmenopausal women. Clin Interv Aging 13: 285-295. https://doi.org/10.2147/CIA.S153782

Ruff KJ, DeVore DP (2014) Reduction of pro-inflammatory cytokines in rats following 7-day oral supplementation with a proprietary eggshell membrane-derived product. Mod Res Inflamm 3(1): 19–25. https://doi.org/10.4236/mri.2014.31003

Saleem A, Saleem M, Akhtar MF (2020) Antioxidant, anti-inflammatory and antiarthritic potential of *Moringa oleifera* Lam: An ethnomedicinal plant of Moringaceae family. S Afr J Bot 128: 246–256. https://doi.org/10.1016/j.sajb.2019.11.023

Schnieders MJ, Kaoud TS, Yan C, Dalby KN, Ren P (2012) Computational insights for the discovery of non-ATP competitive inhibitors of MAP kinases. Curr Pharm 18(9): 1173-1185. https://doi.org/10.2174/138161212799436368

Seemakhan S, Srisook K (2014) *Ageratum conyzoides* leaf extract inhibits inflammatory response via suppression of NF-NB and MAPKs pathway in LPS-induced macrophages. Conference Proceedings. The 5th International Conference on Natural Products for Health and Beauty, Phuket, Thailand, May 6-8, pp. 158–163.

Serhan CN, de la Rosa X, Jouvene C (2019) Novel mediators and mechanisms in the resolution of infectious inflammation: Evidence for vagus regulation. J Intern Med 286(3): 240-258. https://doi.org/10.1111/joim.12871

Sharma V, Holmes JH, Sarkar IN (2016) Identifying complementary and alternative medicine usage information from internet

resources. A systematic review. Methods Inf Med 55(4): 322-332. https://doi.org/10.3414/ME15-01-0154

Shi Y, Zhou K, Li D, Guyonnet V, Hincke MT, Mine Y (2021) Avian eggshell membrane as a novel biomaterial: A review. Foods 10(9): 2178. https://doi.org/10.3390/foods10092178

Sim WJ, Ahn J, Lim W, Son DJ, Lee E, Lim TG (2023) Anti-skin aging activity of eggshell membrane administration and its underlying mechanism. Mol Cell Toxicol 19: 165–176. https://doi.org/10.1007/s13273-022-00291-5

Soehnlein O, Steffens S, Hidalgo A, Weber C (2017) Neutrophils as protagonists and targets in chronic inflammation. Nat Rev Immunol 17(4): 248-261. https://doi.org/10.1038/nri.2017.10

Son ES, Park JW, Kim SH, Park HR, Han W, Kwon OC, Nam JY, Jeong SH, Lee CS (2020) Anti-inflammatory activity of 3,5,6,7,3',4'-hexamethoxyflavone via repression of the NF-κB and MAPK signaling pathways in LPS-stimulated RAW264.7 cells. Mol Med Rep 22(3): 1985-1993. https://doi.org/10.3892/mmr.2020.11252

Stockley RA (1999) Neutrophils and protease/antiprotease imbalance. Am J Respir Crit Care Med 160(5 Pt 2): S49-52. https://doi.org/10.1164/ajrccm.160.supplement_1.13

Sukmawan YP, Alifiar I, Nurdianti L, Ningsih WR (2021) Wound healing effectivity of the ethanolic extracts of *Ageratum conyzoides* L. leaf (white and purple flower type) and *Centella asiatica* and astaxanthin combination gel preparation in animal model. Turk J Pharm Sci 18(5): 609-615. https://doi.org/10.4274/tjps.galenos.2021.34676

Sun X, Zhang Y, Zhou Y, Lian X, Yan L, Pan T, Jin T, Xie H, Liang Z, Qiu W, Wang J, Li Z, Zhu F, Sui X (2022) NPCDR: natural product-based drug combination and its disease-specific molecular regulation. Nucleic Acids Res 50(D1): D1324-D1333. https://doi.org/10.1093/nar/gkab913

Tambunan AP, Bahtiar A, Tjandrawinata RR (2017) Influence of extraction parameters on the yield, phytochemical, TLC-densitometric quantification of quercetin, and LC-MS profile, and how to standardize different batches for long term from *Ageratum conyoides* L. leaves. Pharmacogn J 9(6): 767–774. https://doi.org/10.5530/pj.2017.6.121

Thomford NE, Senthebane DA, Rowe A, Munro D, Seele P, Maroyi A, Dzobo K (2018) Natural products for drug discovery in the 21st century: Innovations for novel drug discovery. Int J Mol Sci 19(6): 1578. https://doi.org/10.3390/ijms19061578

Tian S, Wang J, Li Y, Li D, Xu L, Hou T (2015) The application of in silico drug-likeness predictions in pharmaceutical research. Adv Drug Deliv Rev 86: 2-10. https://doi.org/10.1016/j.addr.2015.01.009

Uhegbu FO, Imo C, Onwuegbuchulam CH (2016) Lipid lowering, hypoglycemic and antioxidant activities of *Chromolaena odorata* (L) and *Ageratum conyzoides* (L) ethanolic leaf extracts in albino rats. J Med Plants Stud 4(2): 155–159.

Vigil de Mello SV, da Rosa JS, Facchin BM, Luz AB, Vicente G, Faqueti LG, Rosa DW, Biavatti MW, Fröde TS (2016) Beneficial effect of *Ageratum conyzoides* Linn (Asteraceae) upon inflammatory response induced by carrageenan into the mice pleural cavity. J Ethnopharmacol 194: 337-347. https://doi.org/10.1016/j.jep.2016.09.003

Vikasari SN, Sukandar EY, Suciati T, Adnyana IK (2022) Antiinflammation and antioxidant effect of ethanolic extract of *Ageratum conyzoides* leaves. IOP Conf Ser: Earth Environ Sci 1104(1): 012024. https://doi.org/10.1088/1755-1315/1104/1/012024

Vikasari SN, Sukandar EY, Suciati T, Adnyana IK (2024) Anti-inflammatory effects of eggshell membrane hydrolysates on carrageenan-induced rat. Pharm Educ 24(2): 152–157. https://doi.org/10.46542/pe.2024.242.152157

Vuong TT, Rønning SB, Suso HP, Schmidt R, Prydz K, Lundström M, Moen A, Pedersen ME (2017) The extracellular matrix of eggshell displays anti-inflammatory activities through NF-κB in LPS-triggered human immune cells. J Inflamm Res 10: 83-96. https://doi.org/10.2147/JIR.S130974

Vuong TT, Rønning SB, Ahmed TAE, Brathagen K, Høst V, Hincke MT, Suso HP, Pedersen ME (2018) Processed eggshell membrane powder regulates cellular functions and increase MMP-activity important in early wound healing processes. PLoS ONE 13(8): e0201975. https://doi.org/10.1371/journal.pone.0201975

Wang CZ, Moss J, Yuan CS (2015) Commonly used dietary supplements on coagulation function during surgery. Medicines (Basel) 2(3): 157-185. https://doi.org/10.3390/medicines2030157

Webb BCW, Rafferty S, Vreugdenhil AJ (2022) Preparation and characterization of antibacterial films with eggshell-membrane biopolymers incorporated with chitosan and plant extracts. Polymers 14(3): 383. https://doi.org/10.3390/polym14030383

Wedekind KJ, Ruff KJ, Atwell CA, Evans JL, Bendele, AM (2017) Beneficial effects of natural eggshell membrane (NEM) on multiple indices of arthritis in collagen-induced arthritic rats. Mod Rheumatol 27(5): 838–848. https://doi.org/10.1080/14397595.2016.1259729

Yadav N, Ganie SA, Singh B, Chhillar AK, Yadav SS (2019) Phytochemical constituents and ethnopharmacological properties of *Ageratum conyzoides* L. Phytother Res 33(9): 2163-2178. https://doi.org/10.1002/ptr.6405

Yang Y, Kim SC, Yu T, Yi YS, Rhee MH, Sung GH, Yoo BC, Cho JY (2014) Functional roles of p38 mitogen-activated protein kinase in macrophage-mediated inflammatory responses. Mediators Inflamm 2014: 352371. https://doi.org/10.1155/2014/352371

Yoo J, Park K, Yoo Y, Kim J, Yang H, Shin Y (2014) Effects of egg shell membrane hydrolysates on anti-inflammatory, anti-wrinkle, anti-microbial activity and moisture-protection. Korean J Food Sci Anim Resour 34(1): 26-32. https://doi.org/10.5851/kosfa.2014.34.1.26

Yuan H, Ma Q, Ye L, Piao G (2016) The traditional medicine and modern medicine from natural products. Molecules 21(5): 559. https://doi.org/10.3390/molecules21050559

Zhu L, Ma M, Ahn DU, Guyonnet V, Wang L, Zheng Y, He Q, Xiong H, Huang X (2022a) Hatched eggshell membrane can be a novel source of antioxidant hydrolysates to protect against H_2O_2-induced oxidative stress in human chondrocytes. Antioxidants (Basel) 11(12): 2428. https://doi.org/10.3390/antiox11122428

Zhu L, Xiong H, Huang X, Guyonnet V, Ma M, Chen X, Zheng Y, Wang L, Hu G (2022b) Identification and molecular mechanisms of novel antioxidant peptides from two sources of eggshell membrane hydrolysates showing cytoprotection against oxidative stress: A combined *in silico* and *in vitro* study. Food Res Int 57: 111266. https://doi.org/10.1016/j.foodres.2022.111266

Zuo HL, Huang HY, Lin YC, Cai XX, Kong XJ, Luo DL, Zhou YH, Huang HD (2022) Enzyme activity of natural products on cytochrome P450. Molecules 27(2): 515. https://doi.org/10.3390/molecules27020515

AUTHOR CONTRIBUTION:

Contribution	Vikasari SN	Sukandar EY	Suciati T	Adnyana IK
Concepts or ideas	x	x	x	x
Design	x	x	x	x
Definition of intellectual content	x	x	x	x
Literature search	x			x
Experimental studies	x			x
Data acquisition	x			x
Data analysis	x			x
Statistical analysis	x			x
Manuscript preparation	x	x	x	x
Manuscript editing	x	x	x	x
Manuscript review	x	x	x	x

Citation Format: Vikasari SN, Sukandar EY, Suciati T, Adnyana IK (2024) Anti-inflammatory effect of the mixture of *Ageratum conyzoides* L. extract and eggshell membrane hydrolysates and *in silico* active compound predictions. J Pharm Pharmacogn Res 12(5): 972–993. https://doi.org/10.56499/jppres24.1956_12.5.972